SKBF
KBS
TEKNISK
RAPPORT
80-22

Evaluation of five glasses and glass-ceramic for solidification of Swedish nuclear waste

Larry L Hench
Lagawan Urwongse

Ceramics Division
Department of Materials Science and Engineering
University of Florida, Gainesville, Florida 1980-08-16

SVENSK KÄRNBRÄNSLEFÖRSÖRJNING AB / PROJEKT KÄRNBRÄNSLESÄKERHET

POSTADRESS: Kärnbränslesäkerhet, Box 5864, 102 48 Stockholm, Telefon 08-67 95 40

EVALUATION OF FIVE GLASSES AND A GLASS-CERAMIC FOR SOLIDIFICATION OF SWEDISH NUCLEAR WASTE

Larry L Hench
Ladawan Urwongse

Ceramics Division
Department of Materials Science and Engineering
University of Florida, Gainesville, Florida

1980-08-16

A list of other reports published in this series is attached at the end of this report. Information on KBS technical reports from 1977-1978 (TR 121) and 1979 (TR 79-28) is available through SKBF/KBS.

EVALUATION OF FIVE GLASSES AND A GLASS-CERAMIC FOR SOLIDIFICATION OF SWEDISH NUCLEAR WASTE

by

Prof. Larry L. Hench and Dr Ladawan Urwongse
Ceramics Division
Dept. of Materials Science and Engineering
University of Florida
Gainesville
FLORIDA
32611 U.S.A.

EVALUATION OF FIVE GLASSES AND A GLASS CERAMIC FOR SOLIDIFICATION OF SWEDISH NUCLEAR WASTE

SUMMARY

A study of the relative leaching resistance four borosilicate glasses, one alkali-alkaline earth alumino-silicate glass and one crystallized glass or glass ceramic has been performed. All six materials had a simulated waste loading of $9^{w}/o$ and a low melting temperature, $< 1150^{o}$ C, required for the French AVM process. The findings were: Leach rates of zinc borosilicate glasses in 90^{o}C deionized water are in the range $5 \times 10^{-7} - 5 \times 10^{-6}$ g/cm^2 day for Na^{+} and Si^{4+}. These values are better than for soda-borosilicate glasses ($1\text{-}5 \times 10^{-5}$ g/cm^2 day). Increasing the Fe_2O_3 content in either sodaborosilicate glasses or zinc borosilicate glasses improves the leach resistance by a factor of 3-5. Fe_2O_3 additions appear to concentrate within the surface films as leaching proceeds.

The alkali-alkaline earth-alumino-silicate glass had a leach resistance nearly equivalent to a high Fe_2O_3 zinc borosilicate glass. However, a crystallization of that glass seriously degraded its leach resistance, apparently due to attack of a residual vitreous phase in the grain boundaries which concentrates alkali ions.

The leach resistance of alkali borosilicate glasses, zinc borosilicate glasses and alkali-alkaline earth-alumino

silicate glasses was not sensitive to surface area to solution volume (SA/V) ratios 0.01 cm^{-1} to 100 cm^{-1}. This was apparently because loss of amphoteric ions into solution prevented the solution pH from becoming alkaline and attacking the glass network more rapidly at high SA/V ratios.

Introduction

The purpose of this study was to evaluate the relative leaching resistance of five glass compositions and one crystallized glass or glass-ceramic that are under consideration for use in the solidification of Swedish nuclear waste. All compositions are compatible with the low melting temperature, $\lesssim 1150^{\circ}C$, required for the French AVM process. A unique feature of the glasses and glass-ceramic studied is the 9 weight percent limit on simulated waste products included in the materials. The 9 w/o limit is characteristic of the Swedish nuclear waste program and potentially provides more latitude in the selection of glass formulations than higher percentage loadings. Thus, lower leaching rates may be possible with glasses that have a lower percentage of waste products than previously reported.

Materials Preparation

The materials studied (Table I) include two soda borosilicate glasses (Nos 1 and 2) and two zinc borosilicate glasses (Nos 3 and 4) with both pairs differing in iron oxide content. Glass No 5 is a low melting (400 poise at 1058°C) alkali-alkaline earth-alumino-silicate glass and sample No 6 is a crystallized material of the same composition as No 5.

Compositions Nos 1, 2 and 3 in Table I were prepared in the author's laboratory by melting at 1150°C in refractory crucibles for 4 hours followed by casting into 10 cm x 1 cm x 1 cm blocks. After annealing at 500°C for 4 hours the blocks were sliced into approximately 2 mm thick samples using a diamond bladed wafering saw operating at moderate speed with acetone as a coolant and lubricant. The as-cut samples were dry polished with 320 and 600 grit SiC paper. The composition used for the 9 % waste simulation in glasses No 1, 2 and 3 is given in Table II.

Materials No 4, 5 and 6 (Tables I, II) were prepared in a similar manner to that described above by T. Lakatos of the Glass Research Institute, Växjö, Sweden. Sample No 6 had a composition equivalent to sample No 5 but was crystallized by heating for 64 hours at 900°C. Nine weight percent of a similar simulated waste composition (Table II) was added to samples No 4, 5 and 6.

Leaching Procedure

The procedure followed in the leaching experiments was similar to that described in the U.S. Dept. of Energy, Materials Characterization test MCC-1 (1). The configuration and dimensions of the static leaching cells and test specimens is shown in Figure 1. Four different sized polyethylene or teflon containers were used in order to vary the ratio of glass surface area (SA in cm^2) to solution volume (V in cm^3), SA/V in cm^{-1}, over a range from 0.1 cm^{-1} to 100 cm^{-1}. This wide range of SA/V was selected for investigation because other studies have indicated that the dependence of leaching behavior of glasses on SA/V can be related to the mechanisms of leaching, long term performance of glasses (2), and the possible range of predictable behavior of nuclear waste solids (3). It is also possible that wide ranges of SA/V ratios may be important in predicting the performance of glass in various transportation or storage accident scenarios where glass fracture or large variations in volume of water are involved.

For conditions involving large volumes of solution the samples were suspended with nylon string. In conditions of SA/V=1.0 cm^{-1} the samples were placed at an angle in the solution with only two edges touching the sides. To achieve the high SA/V$\approx$100cm^{-1} conditions the samples were placed in a stacked configuration such that their faces were in contact. This produces an SA/V ratio of approximately 100 cm^{-1} according to previous studies (4). However, this configuration results in only an approximate SA/V value and therefore no quantitative solution analyses are reported. Surface analyses of the leached glasses are possible though.

Containers containing the samples and deionized water, initial pH=6.5, were maintained at 90°C ±0.5°C using a controlled water bath. After the leaching times indicated, the containers were removed, the samples rinsed with acetone and infrared reflection analyses of the surfaces were made. The pH of the solutions was measured and the Si, B and Al concentrations determined using colorimetry. Analyses of Na, Mn, Mo, Fe and Cs were obtained using atomic absorption and atomic emission spectroscopy.

Weight losses were monitored throughout the experiment but they were too variable to be reported.

Infrared Reflection Spectroscopic (IRRS) Analysis

IRRS spectra were obtained to compare changes in the specimen surface due to leaching. Interpretation of the IRRS spectral changes for these samples is illustrated in Fig. 2. A fused silica standard is shown in the top half of Fig. 2 for purposes of calibration and comparison with the experimental glasses. The primary peak of fused silica is located at approximately 1100 cm^{-1} and is due to silicon-bridging oxygen-silicon stretching vibrations (5). A second major peak of fused silica is located at approximately 450 cm^{-1} that is due to bridging silicon-oxygen-silicon rocking vibrations. Most interpretation of surface corrosion of glasses is based upon changes in the stretching vibration peak as shown in previous publications (4, 6).

The spectrum of glass No 1 before corrosion is shown as a full line in the top half of Fig. 2. The spectral intensity in the region between 800 cm^{-1} and 900 cm^{-1} is due to the presence of silicon-non-bridging oxygen-alkali and alkaline earth ions. When corrosion of the surface occurs, the exchange of alkali and alkaline earth cations with hydrogen ions reduces the intensity of that portion of the spectral region. This phenomena is shown by the dashed curve in the top half of Fig. 2 which is obtained on glass No 1 after one day corrosion at 90°C with SA/V of 0.1 cm^{-1}. The peak that remains in the spectrum located around 1100 cm^{-1} is due to the formation of a silica-rich film on the surface of the glass.

Thus, changes in the IRRS spectra can be used to monitor the rate of loss of the alkali from the surface

of the sample and the formation of a silica-rich film. For either longer corrosion times or higher surface area to volume ratios, which may produce a faster reaction, the IRRS intensity is reduced even further by gradually destroying the surface film that forms on the glass. This produces a roughening of the surface and scattering of the infrared beam incident on the sample. This phenomena is illustrated in the curve shown with the dot-dash sequence in the top half of Fig. 2.

The same glass (No 1) leached for the same time and temperature shows a more severe surface attack and loss of IRRS intensity when the SA/V ratio is increased by a factor of 100 (compare the curves for SA/V=0.01 cm^{-1} and 1.0 cm^{-1}). As will be shown below, this is due to an increase in solution pH at the higher SA/V valves for this glass which results in an attack of the SiO_2-rich film and roughens the surface (4, 6).

Thus, different glass compositions or differing corrosion conditions can be compared by examining both the loss of alkali related regions from IRRS-spectra, formation of films on the surface of the samples, and destruction of the films and subsequent roughening of the surface.

An illustration of the difference observed between a poorly durable glass, such as glass No 1, and a glass of high durability such as glass No 3, is shown in the bottom half of Fig. 2. The full curve is the spectrum for glass No 3 before leaching. There is little apparent difference in the original spectra between glass 1 and 3 before leaching. However, after one day leaching at $90^{o}C$ at SA/V = 1.0 cm^{-1} the dot-dash curve for glass No 3 shows almost no change other

than a slight increase in intensity generally due to the formation of a very thin, high durability film on the glass surface. In contrast, the glass No 1 spectrum has already gone through formation of a non-protective surface film and attack of the film to a roughened surface. As will be shown later, this change is due to a large difference in the rate of alkali and other mobile species released from the surface and the accompanying rise in the pH of the solution. As is also shown in the bottom half of Fig. 2, glass No 3 continues to form a silica rich film on the surface. This is shown by the 7 day spectrum with a surface area to volume condition of 0.01 cm^{-1}. It is the use of such changes in spectra that are the basis for comparing the performance of the 6 materials in this study.

Results

Table III presents the pH of the leaching solution and the parts per million (ppm) of ions measured in the solution for the various ratios of surface area to solution volume (SA/V) and leaching times investigated. Values of high SA/V solutions were restricted to only a few elements in many cases because of the small quantities of liquid used in the experiment. A few values are also not present because of evaporation of liquid from the containers.

Leaching rates in units of grams/cm^2/day are given in Table IV for several of the elements leached at SA/V = 0.1 cm^{-1}. Leach rates and surface analyses are shown only for the SA/V = 0.1 cm^{-1} condition for the sake of brevity. The 0.1 cm^{-1} value was chosen because it is in the middle of the SA/V range that is experimentally accessible.

The change in pH with leaching time at SA/V = 0.1 cm^{-1} is compared for the six materials in Fig. 3. The alkali borosilicate glasses (Nos 1, 2) produce a higher solution pH than the zinc borosilicate glasses (Nos 3, 4). In both types of composition the presence of Fe_2O_3 in the glass significantly reduces both the magnitude of solution pH and the time dependence of the pH change.

The alkali-alkaline earth-alumino-silicate glass (No 5) shows a progressive decrease of pH with time. Crystallization of the glass (No 6), however, results in a material that generates a rapid rise in pH which continues throughout the 28 day period studied.

Figures 4, 5 and 6 show the time dependence of the Na^+,

SiO_2 and B^{3+} leach rates calculated from the SA/V = 0.1 cm^{-1} solution data. Leach rates for all compositions tend to decrease for the first 14 days with in some cases an decrease at 28 days.

Glasses Nos 1, 2 and glass-ceramic No 6 generally exhibit the highest leach rates with values for Na^+ and SiO_2 being in the range of 1 to 5 x 10^{-5} g/cm^2/day after 14 days. Glass No 4 is intermediate with leach rates of ~5 x 10^{-6} g/cm^2/day and glasses No 3 and No 5 are generally lowest, being in the range of 5 x 10^{-7} to 1 x 10^{-6} g/cm^2/day. Thus, relatively small changes in parent glass composition can increase leach resistance by nearly a factor of 100 when the waste loading is a constant 9 % by weight.

Comparison of leaching results for the various SA/V ratios studied did not show any systematic dependence of leach rates on this experimental parameter. The time dependence of solution pH also did not exhibit any marked variation with differing SA/V values (Table III). For example, glasses Nos 3, 4 and 5 that show a decrease in pH with time do so independent of low or high SA/V ratios.

The data of Table III show very little Al^{3+} or Fe^{3+} in solution. Multiple valence Mn and Mo ions also show very low concentrations in solution. No systematic dependence of SA/V is apparent for the leach rates of these ions either. Compositions that show the higher leach rates for major constituents, such as samples Nos 1, 2 and 6, also exhibit the most marked loss of Mo, Mn and Co which are representative of radionuclides in active waste. The loss of these ions from the better materials is very low.

Surface analysis of the samples after leaching showed marked differences between the six materials even though the solution leach rates were similar in some cases. Figures 7 - 11 compare the time dependent changes in IRRS spectra after leaching at SA/V = 0.1 cm^{-1}. Before leaching, Fig. 7, there are small variations in the spectra of the six materials primarily due to the lower content of network formers such as SiO_2 and B_2O_3 in samples Nos 5 and 6.

After leaching for just 1 day at 90°C large differences in leach resistance are apparent (Fig. 8). Glass No 1 and glass-ceramic No 6 show a loss in IRRS intensity throughout the 1100 - 800 cm^{-1} region, corresponding to an overall roughening of the surface, and are definitely the most severely damaged by the leaching.

Glasses No 2 and No 4 have lost intensity only in the 1000 - 800 cm^{-1} region, which indicates depletion of alkali ions from the surface and formation of a silica-rich film (Fig. 8). In contrast, within the 1 day period glasses No 3 and No 5 show little evidence of any surface attack.

Continued exposure of the samples to longer times, Figures 9 - 11, shows a progressive loss of reflected intensity for samples Nos 1, 2, 4 and 6 due to the roughened surface accompanying total network dissolution following dealkalization. By 7 days (Fig. 9) glass No 3 has also shown evidence of dealkalization but has started to form a protective SiO_2-rich film which helps provide a high leach resistance. By day 28 (Fig. 11) some surface roughening and network attack is also evident for glass No 3 however. This produces a slow decrease in intensity in the Si-alkali-non

bridging oxygen region of the spectra (950 cm^{-1}) as shown in Fig. 12. Glasses Nos 1 and 2 show very rapid loss of this portion of the IRRS spectra (Fig. 12). Glass No 4 also shows progressive development of a protective surface layer between days 7 - 28 resulting in a sharp IRRS peak centered around 1050 cm^{-1} (Figures 10 - 11). The increase in this peak with time as well as an increase in the 950 cm^{-1} region (Fig. 13) suggests that ions previously in solution may becoming incorporated in the surface layer.

Glass No 5 still shows little change in any portion of the IRRS spectra even after 28 days leaching (Fig. 11). The 950 cm^{-1} region of the spectrum most sensitive to to dealkalization, the initial stage of attack, shows little decrease in intensity with duration of leaching.

In order to compare the relative depths of the sample surface affected by leaching at SA/V = 0.1 cm^{-1} IRRS profiles of the two most leach resistant samples, Nos 3 and 5, were obtained. Several μm of material were removed from the surface of the leached samples by dry mechanical polishing with 600 grit SiC paper. The samples were weighed before and after each polishing step and IRRS spectra taken. The thickness of the layer removed was estimated from the change in weight by assuming a density of 2.2 g/cm^3. Because the actual density of the surface film removed is unknown, the calculated thicknesses may be uncertain to ± 25 %.

Fig. 14 shows the spectral changes resulting from progressive removal of layers approximately 0.002 cm thick from glass No 3 after 28 day leaching. A total thickness of 0.012 cm was removed before the original,

unleached spectrum of the surface was restored.

Surface reaction profiles for glasses Nos 3 and 5 are compared in Fig. 15. The depth of surface affected by the aqueous attack was less than 0.006 cm for glass No 5, approximately one-half that of glass No 3.

Variations in SA/V ratios have only a minor effect on the nature of surface attack of the various compositions. Fig. 16 compares IRRS spectra after 7 days leaching of glasses Nos 3 and 4 over a SA/V range of $\sim$1000. Glass No 5 is not shown because almost no differences were detected. Both glasses Nos 3 and 4 show a somewhat enhanced tendency to produce a silica-rich reaction layer at the low SA/V values. This difference cannot be related to general pH effects because of the stable pH response to the various SA/V values. However, it may be related to effects of ion diffusion and depletion in the larger solution volumes which permit a more rapid alkali depletion. Any such difference however does not show up in the leach rate dependence on SA/V.

Discussion of Results

Both solution analyses and IRRS surface analyses showed differences between the three types of glasses under consideration. A large difference between the leaching of a glass and glass-ceramic of the same composition was also observed. The soda borosilicate glass with low iron content (No 1) performed poorly in comparison with the other glass compositions. This poor performance was due to a combination of not forming a protective surface film and producing a progressive increase in solution pH which led to an attack of the silica network of the glass surface. The net effect of both of these factors was a leach rate higher by nearly 100 times that of the better compositions in this series.

Increasing Fe_2O_3 content in the glasses at the expense of SiO_2 and B_2O_3 (glass No 2) improves the leach resistance by approximately 3 to 5 times (Tables III and IV). The improvement is apparently due to the development of a more stable surface film at longer times with Fe_2O_3 being incorporated within the film (Figures 9 and 10). This interpretation is based upon the fact that even with a large concentration of Fe_2O_3 in the glass no Fe ions were detectable in the leachant even after 28 days. Similar results were obtained with Al^{3+} in this study (Table III) and it is concluded that Al_2O_3 is built into the surface film as well. Previous investigations involving both Al_2O_3 as a constituent in glass (7) and Al^{3+} in solution (8) showed incorporation of the R^{3+} species into a protective surface film which significantly decreased the rate of aqueous attack of the surface. The present data suggest Fe^{3+}

is behaving in an equivalent manner for these complex nuclear waste glasses. An additional consequence of the presence of the amphoteric Fe ions is the maintenance of a nearly neutral pH in the leachant, Fig. 3, for glass No 2 whereas without the buffering action of the iron ions the proton-alkali exchange results in a continuing increase in hydroxyl ion concentration in the leachant (glass No 1 in Fig. 3).

There was a similar effect of Fe_2O_3 additions on the leaching behavior of the zinc borosilicate glasses, Nos 3 and 4. However, the improvement of leach resistance of glass No 3 to glass No 4 may not be entirely attributable to the addition of Fe_2O_3 because the Na_2O, B_2O_3 and Li_2O were also changed, albeit only a small amount.

Both compositions Nos 3 and 4 produced protective films during leaching, Figures 10 and 11. They also maintained a leachant pH buffered somewhat acidic (Fig. 3) which protects the surface from network dissolution. Glass No 3 exhibited a lower leach rate by about a factor of 5 apparently because of the Fe_2O_3 stabilization of the surface film, as discussed above. Leach rates of 1×10^{-6} g/cm^2/day for both SiO_2 and Na^+ were generally independent of the SA/V range investigated (100 cm^{-1}) which also is indicative that the improvement in leaching behavior is related to a more stable surface film rather than a change in solution chemistry.

Glass composition No 5 represents a major alternative from the alkali borosilicate glasses generally considered for use in nuclear waste solidification. The No 5 alkali-alkaline earth-alumino silicate formula,

developed by T. Lakatos, Swedish Glass Research Institute, has a low melting behavior (400 poise at 1058°C) equivalent to that of the borosilicate glasses. However, composition No 5 does not contain B_2O_3 which contributes to the leaching of the other compositions (Fig. 6).

Leachant solution data show that the resistance of glass No 5 to aqueous attack is excellent with leach rates for SiO and Na^+ in the range of 5×10^{-7} to 1×10^{-6} g/cm /day (Figures 4 and 5). However, over the entire range of times and SA/V range investigated (Table III) there is no systematic trend for the No 5 composition to be superior to the best of the borosilicate glasses investigated (No 3).

Glass No 5 maintains a stable solution pH throughout the times studied primarily because there is very little sodium in the glass to produce a pH rise. A consequence of the low sodium content is the resistance of the glass surface to dealkalization, pitting or roughening, which results in the stable IRRS surface spectra throughout the 28 day period (Figures 8-11, 13). It is also responsible for the very thin reaction film measured with the IRRS profiling technique (Fig. 15). Thus, these results indicate that low melting alkali-alkaline earth-alumino-silicate glasses may be an alternative to borosilicate glasses for use in the solidification of nuclear wastes at a level of 9 % loading by weight. However, the results of leach studies over a wide range of SA/V values up to 28 days at 90°C are approximately equivalent to the zinc borosilicate glass containing Fe_2O_3.

The leaching behavior of the best borosilicate glass from this study (No 3) is quite favorable and in many

conditions tested better than one of the borosilicate reference glasses of the U.S. waste program (PNL 76-68). Table V shows the comparative leach rates obtained over the 28 day period for the two glasses leached under identical conditions. Throughout the first 14 days of testing the leach rates for all three elements listed are lower for glass No 3, in some cases by as much as 50 times. This is very likely a consequence of the much lower percentage of SiO_2 (39.8 w/o) and higher Na_2O (12.8 w/o) content of the 76-68 glass that is associated with a higher waste loading factor.

A major difference in the behavior of the two glasses is the continuing decrease of leach rates with time for 76-68 versus the increase in leach rates between 14 days and 28 days for glass No 3. Since such an increase in leach rates with time is unusual behavior for glasses it is uncertain at this time whether it is characteristic of certain of the glass formulas investigated in this study or some other factor. The IRRS data, Fig. 11, confirms that additional attack has occurred between days 14 and 28 but does not indicate why it should be at a faster rate than at 14 days.

Comparison of the leaching behavior of the glass-ceramic studied (No 6) with a glass of the same composition (No 5) indicates that crystallization was detrimental to performance of the material. Leach rates were as much as 50 - 100 times worse for the glass-ceramic under some conditions. The rapid increase of solution pH for this material, Fig. 3, suggests that the alkali and alkaline earth ions segregated into the grain boundaries during crystallization and led to preferential leaching of a more soluble glass phase. This result indicates that it may be very difficult to produce a

glass-ceramic with controlled resistance to aqueous attack with the wide variability in potential alkali content in nuclear wastes. It also suggests that prolonged cooling of canisters containing large masses of glass and subsequent devitrification of the center of the block could lead to a material with decreased leach resistance. Avoiding crystallization seems to be the best way to minimize this potential problem rather than trying to control crystallization.

Conclusions

1. Leach rates of zinc borosilicate glasses containing 9 weight percent waste loading in 90°C deionized water are approximately 5×10^{-7} g/cm^2/day to 5×10^{-6} g/cm^2/day for Na^+ and Si^{4+}. These values are better than sodaborosilicate glasses with the same waste loadings ($1 - 5 \times 10^{-5}$ g/cm^2/day) tested under identical conditions.

2. Increasing the Fe_2O_3 content in either sodaborosilicate glasses or zinc borosilicate glasses improves leach resistance by a factor of 3 to 5 times.

3. Surface analyses of iron-containing sodaborosilicate glasses and zinc borosilicate glasses show formation of silica-rich films during leaching. Fe_2O_3 additions appear to concentrate within the surface films as leaching proceeds improving film stability and leach resistance.

4. An alkali-alkaline earth-alumino-silicate glass with a 1 percent waste loading has better leach resistance (5×10^{-7} g/cm^2/day - 5×10^{-6} g/cm^2/day) than soda borosilicate glasses ($1 - 5 \times 10^{-5}$ g/cm^2/day) with the same waste loading but is nearly equivalent to a high Fe_2O_3 zinc borosilicate glass.

5. Crystallization of an alkali-alkaline earth-alumino-silicate glass seriously degrades its leach resistance apparently due to attack of a residual vitreous phase in the grain boundaries which concentrates alkali ions.

6. The leach resistance of alkali borosilicate glasses,

zinc borosilicate glasses and alkali-alkaline earth alumine silicate glasses was not sensitive to SA/V ratios from 0.01 cm^{-1} to 100 cm^{-1}. This was apparently because loss of amphoteric ions into solution prevented the solution pH from becoming alkaline and attacking the glass network more rapidly at high SA/V values.

Acknowledgements

The authors gratefully acknowledge the support of Swedish SKBF/Project KBS and the encouragement of Lars Werme throughout the course of this experiment. They also appreciate the assistance of the U.S. Dept. of Energy, Battelle Pacific Northwest Laboratories and Savannah River Labs at several stages. The technical assistance of D.E. Clark, G. McVey, J.W. Hench, S.D. Hench, A.A. Hench, M. Wilson, S. Wilson and J. Greenhalgh is also appreciated.

Table I. Experimental Glass and Glass-Ceramic Compositions (Weight Percent)

Sample	No 1*	No 2**	No 3***	No 4†	No 5††	No 6†††
SiO_2	50.0	48.0	51.6	52.0	42.0	42.0
Al_2O_3	2.1	2.0	2.2	2.5	16.5	16.5
B_2O_3	23.1	22.2	14.5	15.9	0	0
Na_2O	13.6	13.1	8.5	9.4	4.0	4.0
Fe_2O_3	0.6	4.0	4.0	0.6	0.6	0.6
UO_2 or CeO_2	1.66	1.66	1.66	1.7	1.7	1.7
ZnO	-	-	6.0	6.0	6.0	6.0
Li_2O	-	-	1.8	3.0	5.7	5.7
TiO_2	-	-	-	-	3.0	3.0
ZrO_2	-	-	-	-	2.0	2.0
BaO	-	-	-	-	2.5	2.5
CaO	-	-	-	-	7.0	7.0
Simulated Waste Products (See Table II)	9.0	9.0	9.0	9.0	9.0	9.0

* Designated ABS 1

** Designated ABS 19

*** Designated ABS 24

† Designated ABS 29

†† Designated SAC 25

††† Designated SAC 25 - Glass Ceramic Crystallized 900°C/64 min.

Table II. Composition of Simulated Nuclear Waste (Weight Percent)

	Added to Glasses 1, 2, 3	Added to Compositions 4, 5, 6
Cs_2O	9.69	9.78
SrO	2.86	2.89
BaO	5.07	5.11
Y_2O_3	1.65	1.67
ZrO_2	14.10	14.22
MoO_3	17.95	18.11
MnO_2	8.48	8.56
CoO	2.31	-
NiO	4.07	4.11
Ag_2O	0.12	0.12
GdO	0.29	-
SnO	0.15	0.19
Sb_2O_3	0.04	0.04
CeO_2	8.26	-
La_2O_3	7.82	7.89
Nd_2O_3	13.33	13.44
Pr_2O_3	3.85	4.22
Cr_2O_3	-	8.33
NiO	-	4.11
CdO	-	0.29

Table III. Concentration (ppm) of Elements Leached Into Solution

Sample	pH	(ppm) SiO_2	(ppm) Si^{4+}	(ppm) Na^{+}	(ppm) B^{3+}	(ppm) Al^{3+}	(ppm) Mn	(ppm) Mo	(ppm) Fe	(ppm) Cs^{+}
1 Day Corrosion at 90°C										
SA/V = 0.01										
1	4.16	7.25	3.38	0.3	0.2	-	-	-	-	-
2	5.65	4.25	1.98	0.18	0.5	-	-	-	-	-
3	5.25	1.25	0.58	0.05	0	-	-	-	-	-
4	5.58	5.0	2.33	0.10	0	-	-	-	-	-
5	5.23	2.75	1.28	0.05	0	-	-	-	-	-
6	6.43	3.5	1.63	0.1	0	-	-	-	-	-
SA/V = 0.1										
1	6.61	11.0	5.13	1.57	2.7	-	-	-	-	-
2	6.42	5.5	2.56	1.50	1.9	-	-	-	-	-
3	5.17	0.25	0.11	0.20	0.4	-	-	-	-	-
4	6.85	0.25	0.11	0.60	0.6	-	-	-	-	-
5	4.86	0.25	0.11	0.10	0	-	-	-	-	-
6	7.49	11.75	5.48	1.08	0	-	-	-	-	-
SA/V = 1.0										
1	-	250.0	116.65	70.00	40	-	-	-	-	-
2	-	200.0	93.32	19.00	20	-	-	-	-	-
3	-	-	-	2.90	-	-	-	-	-	-
4	-	10.25	4.78	1.50	-	-	-	-	-	-
5	-	17.5	8.16	2.90	1.0	-	-	-	-	-
6	-	75.0	35.0	20.50	5.0	-	-	-	-	-

(Continued)

Note: The dashed lines indicate data not available, usually due to insufficient solution available for all analyses indicated.

Table III (Cont.)

Sample	pH	(ppm) SiO_2	(ppm) Si^{4+}	(ppm) Na^{+}	(ppm) B^{3+}	(ppm) Al^{3+}	(ppm) Mn	(ppm) Mo	(ppm) Fe	(ppm) Cs^{+}
7 Days Corrosion at 90°C										
SA/V = 0.01										
1	6.01	3.0	1.40	0.56	0.4	0	0.03	0	-	-
2	6.16	1.75	0.82	0.40	0.2	0	0.02	0	-	-
3	5.72	0	0	0	0	0	0.02	0	-	-
4	6.51	0.25	0.12	0.20	0	0	0.01	0	-	-
5	5.50	0	0	0	0	0	0.01	0	-	-
6	7.92	11.0	5.13	0.35	0.1	0	0.01	0.3	-	-
SA/V = 0.1										
1	6.78	36.25	16.92	6.7	8.7	0	0.08	0.5	-	-
2	6.47	13.50	6.30	5.0	6.7	0	0.06	0.2	-	-
3	5.19	1.25	0.58	0.5	0.9	0	0.03	0	-	-
4	5.96	0.5	0.23	1.5	2.5	0	0.07	0.2	-	-
5	4.58	1.75	0.82	0	0	0	0.02	0	-	-
6	7.85	28.0	13.07	3.3	0	2	0	1.3	-	-
SA/V = 1.0										
1	8.19	252.5	117.8	62.0	91	-	-	-	-	-
2	7.76	247.5	115.5	57.0	88	-	-	-	-	-
3	6.46	22.5	10.49	3.3	1	-	-	-	-	-
4	6.83	25.0	11.66	3.5	3	-	-	-	-	-
5	7.02	12.5	5.83	3.3	0	-	-	-	-	-
6	8.61	77.5	36.16	30.0	0	-	-	-	-	-

(Continued)

Table III (Cont.)

Sample	pH	(ppm) SiO_2	(ppm) Si^{4+}	(ppm) Na^{+}	(ppm) B^{3+}	(ppm) Al^{3+}	(ppm) Mn	(ppm) Mo	(ppm) Fe	(ppm) Cs^{+}
14 Days Corrosion at 90°C										
SA/V = 0.01										
1	6.75	7.75	3.65	1.1	0.8	0	0.03	0.1	-	-
2	6.44	1.25	0.58	0.5	0.6	0	0.02	0.1	-	-
3	5.15	0	0	0.06	0.2	0	0.02	0	-	-
4	6.01	1.75	0.82	0.15	0.3	0	0.02	0	-	-
5	5.33	0.50	0.23	0	0.2	0	0	0	-	-
6	8.15	21.0	9.80	0.55	0.3	2	0	0.3	-	-
SA/V = 0.1										
1	7.04	29.75	13.88	6.2	8.5	0	0.03	0.4	-	-
2	6.39	10.00	4.67	7.4	5.1	0	0.11	0.1	-	-
3	5.01	1.50	0.70	0.8	0.1	0	0.05	0	-	-
4	5.91	2.5	1.17	1.8	2.1	0	0.08	0.1	-	-
5	4.17	0.75	0.35	0.5	0	0	0.05	0	-	-
6	7.86	39.0	18.20	3.4	0	2	0.01	1.6	-	-
SA/V = 1.0										
1	7.27	575	268.0	230.0	-	-	-	-	-	-
2	4.91	295	137.7	85.0	140	-	-	-	-	-
3	-	-	-	-	-	-	-	-	-	-
4	-	125	58.32	3.3	4	-	-	-	-	-
5	-	25	11.66	2.0	0	-	-	-	-	-
6	-	200	93.3	-	0	-	-	-	-	-

(Continued)

Table III (Cont.)

Sample	pH	(ppm) SiO_2	(ppm) Si^{4+}	(ppm) Na^{+}	(pmm) B^{3+}	(ppm) Al^{3+}	(ppm) Mn	(ppm) Mo	(ppm) Fe	(ppm) Cs^{+}
28 Days Corrosion at 90°C										
SA/V = 0.01										
1	6.35	22.5	10.49	1.75	1.2	0	0.06	0.2	0	1.1
2	5.71	7.5	3.49	0.67	0.3	0	0.02	0	0	0
3	3.16	4.25	1.98	0.20	0	0	0	0	0	0
4	5.71	5.25	2.68	0.24	0.2	0	0.02	0	0	1.0
5	4.67	10.0	4.66	0	0	0	0	0	0	0.9
6	7.67	9.75	4.55	0.52	0	0	0.01	0.5	0	1.0
SA/V = 0.1										
1	8.07	412.5	192.5	47.0	42	0	0.01	0.9	0	1.8
2	6.46	30.0	14.0	13.2	4	0	0.16	0.6	0	0
3	4.90	60.0	28.0	4.8	2	0	0.06	0	0	0
4	5.75	52.5	24.5	6.2	3	0	0.09	0	0	1.1
5	4.19	70.0	32.67	3.8	0	0	0.03	0	0	0.9
6	7.98	27.5	12.83	4.8	0	2	0	2.2	0	0
SA/V = 1.0										
1	7.86	350.0	163.34	132.0	270	-	-	-	-	-
2	7.49	425.0	198.34	113.0	150	-	-	-	-	-
3	5.76	225.0	105.0	10.0	20	-	-	-	-	-
4	6.48	75.0	35.0	13.0	20	-	-	-	-	-
5	5.45	275.0	178.3	10.0	0	-	-	-	-	-
6	-	-	-	-	0	-	-	-	-	-

Table IV. Leaching rates in 90°C H_2O at SA/V = 0.1 cm^{-1}

Sample	SiO_2	Si^{4+}	Na^+	B^{3+}
1 day leach rates ($g/cm^2/day$)				
1	1.1×10^{-4}	5.1×10^{-5}	1.6×10^{-5}	2.7×10^{-5}
2	5.5×10^{-5}	2.6×10^{-5}	1.5×10^{-5}	1.9×10^{-5}
3	2.5×10^{-6}	1.1×10^{-6}	2.0×10^{-6}	4.0×10^{-6}
4	2.5×10^{-6}	1.1×10^{-6}	6.0×10^{-6}	6.0×10^{-6}
5	2.5×10^{-6}	1.1×10^{-6}	1.0×10^{-6}	0
6	1.2×10^{-4}	5.5×10^{-5}	1.1×10^{-5}	0
7 day leach rates ($g/cm^2/day$)				
1	5.2×10^{-5}	2.4×10^{-5}	9.6×10^{-6}	1.2×10^{-5}
2	1.9×10^{-5}	9.0×10^{-6}	7.1×10^{-6}	9.6×10^{-6}
3	1.8×10^{-6}	8.3×10^{-7}	7.1×10^{-7}	1.3×10^{-6}
4	7.1×10^{-7}	3.3×10^{-7}	2.1×10^{-6}	3.6×10^{-6}
5	2.5×10^{-6}	1.2×10^{-6}	---	---
6	4.0×10^{-5}	1.9×10^{-5}	4.7×10^{-6}	---
14 day leach rates ($g/cm^2/day$)				
1	2.1×10^{-5}	9.9×10^{-6}	4.4×10^{-6}	6.1×10^{-6}
2	7.1×10^{-6}	3.3×10^{-6}	5.3×10^{-6}	3.6×10^{-6}
3	1.1×10^{-6}	5.0×10^{-7}	5.7×10^{-7}	7.1×10^{-8}
4	1.8×10^{-6}	8.4×10^{-7}	1.3×10^{-6}	1.5×10^{-6}
5	5.4×10^{-7}	2.5×10^{-7}	3.6×10^{-7}	---
6	2.8×10^{-5}	1.3×10^{-5}	2.4×10^{-6}	---
28 day leach rates ($g/cm^2/day$)				
1	1.5×10^{-4}	6.9×10^{-5}	1.7×10^{-5}	1.5×10^{-5}
2	1.1×10^{-5}	5.0×10^{-6}	4.7×10^{-6}	1.4×10^{-6}
3	2.1×10^{-5}	1.0×10^{-5}	1.7×10^{-6}	7.1×10^{-7}
4	1.9×10^{-5}	8.8×10^{-6}	2.2×10^{-6}	1.1×10^{-6}
5	2.5×10^{-5}	1.2×10^{-5}	1.4×10^{-6}	0
6	9.8×10^{-6}	4.6×10^{-6}	1.7×10^{-6}	0

Table V. Comparison of Leach Rates ($g/cm^2/day$) of a U.S. Reference Borosilicate Glass (PNL 76-68) with the High Fe_2O_3 Zinc Borosilicate Glass No 3 Leached in Deionized Water at 90^oC, SA/V = o.1 cm^{-1}

	Si^{4+}	Na^{+}	B^{3+}
1 Day			
76-68	2.2×10^{-5}	8.5×10^{-6}	1.1×10^{-5}
No 3	1.1×10^{-6}	2.0×10^{-6}	4.0×10^{-6}
7 Days			
76-68	1.3×10^{-5}	3.9×10^{-6}	5.7×10^{-6}
No 3	8.3×10^{-7}	7.1×10^{-6}	1.3×10^{-6}
14 Days			
76-68	1.0×10^{-5}	3.2×10^{-6}	3.5×10^{-6}
No 3	5.0×10^{-7}	5.7×10^{-7}	7.1×10^{-8}
28 Days			
76-68	6.1×10^{-6}	3.4×10^{-6}	2.3×10^{-6}
No 3	1.0×10^{-5}	1.7×10^{-6}	7.1×10^{-7}

References

(1) MCC-1 Static Leach Test, Materials Characterization Center Report, Pacific Northwest Laboratories, 1980

(2) D.E. Clark, E.C. Ethridge and L.L. Hench "Effects of Glass Surface Area to Solution Volume Ratio on Glass Corrosion", Phys. and Chem. of Glasses, 20 (2) (1979) 35-40

(3)a. L.L Hench, D.E. Clark, E. Lue Yen-Bower; Proc. of Conf. on High Level Radioactive Solid Waste Forms; L.A. Casey, ed. NUREG/CP-0005, pub. by U.S./NRC (1979) 199-235

(3)b. L.L. Hench, D.E. Clark, E. Lue Yen-Bower, "Corrosion of Glasses and Glass-Ceramics", Nuclear and Chemical Waste Management, 1, (1980) 59-75

(4) D.E. Clark, L.G. Pantano and L.L. Hench, "Corrosion of Glass", Magazines for Industry, N.Y., New York (1979)

(5) D.M. Sanders, W.B. Person and L.L. Hench, "Quantitative Analysis of Glass Structure Using Infrared Reflection Spectra", Appl. Spectroscopy, 28 (3), (1974) 247-255

(6) D.M. Sanders and L.L. Hench, "Mechanisms of Glass Corrosion", T. Amer. Ceram. Soc., 56 (7), (1973) 373-377

(7) M.F. Dilmore, D.E. Clark and L.L. Hench, "Aqueous Corrosion of Lithia-Alumina-Silika Glasses", Bull. Amer. Ceram. Soc., 57 (1978) 1040-1044

(8) M.F. Dilmore, D.E. Clark and L.L. Hench, "Corrosion Behavoir of Lithia Disilicate Glass in Aqueous Solutions of Aluminum Compounds", Bull. Amer. Ceram. Soc., 58 (11) (1979) 1111-1114

(9) R. Bonniaud, F. Pacaud and C. Sombret "Quelques aspects de comportement de radioelement confinés à long terme sous forme de verre ou de produit à fort phase vitreuse", Verres et Refractaires, Vol 29.1, Jan.-Fev., 1975

(10) J.E. Mendel, "Annual Report on the Characteristics of High Level Waste Glasses", BNWL-2252, June 1977

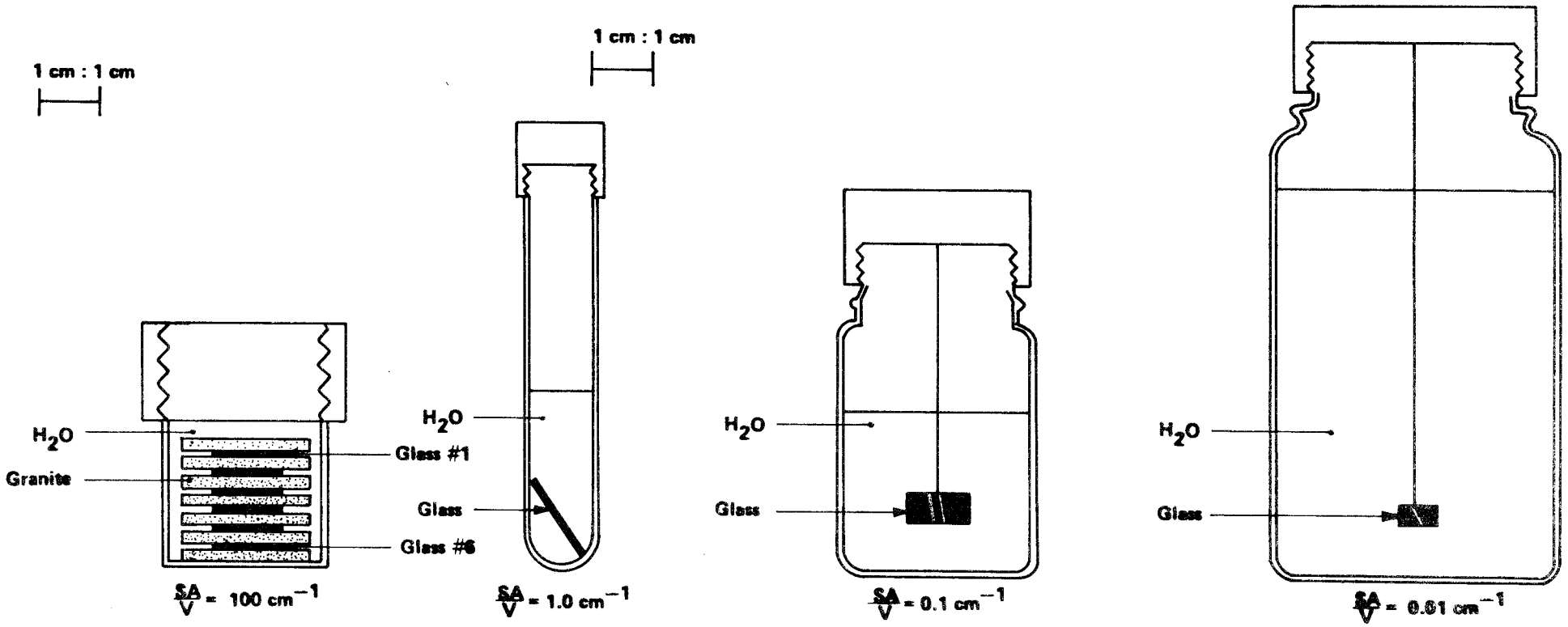
1 cm : 1 cm
H_2O
Granite
Glass #1
Glass #6
$\frac{SA}{V}$ = 100 cm^{-1}
1 cm : 1 cm
H_2O
Glass
$\frac{SA}{V}$ = 1.0 cm^{-1}
H_2O
Glass
$\frac{SA}{V}$ = 0.1 cm^{-1}
H_2O
Glass
$\frac{SA}{V}$ = 0.01 cm^{-1}

Figure 1

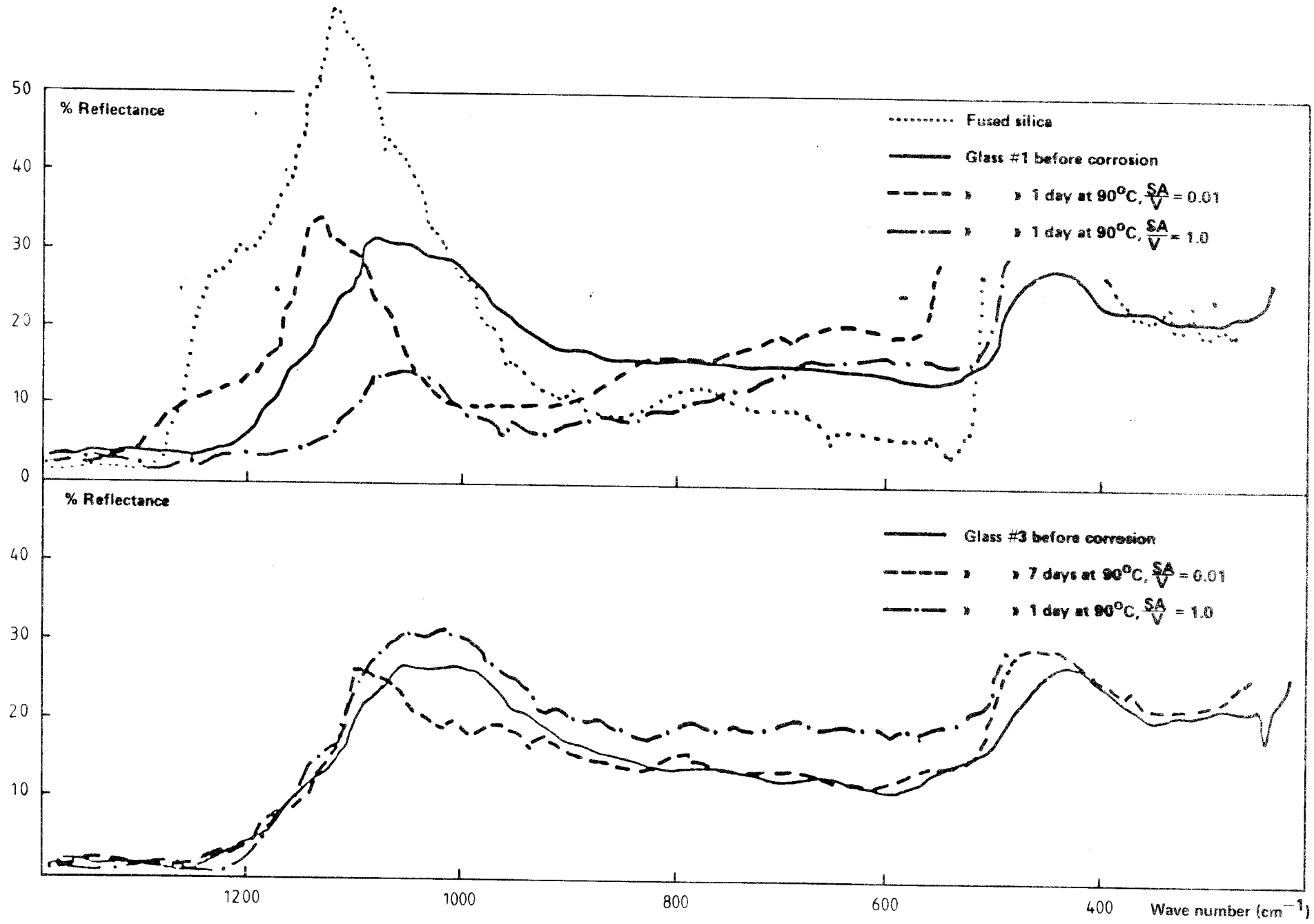
% Reflectance
Fused silica
Glass #1 before corrosion
» » 1 day at 90°C, SA/V = 0.01
» » 1 day at 90°C, SA/V = 1.0
% Reflectance
Glass #3 before corrosion
» » 7 days at 90°C, SA/V = 0.01
» » 1 day at 90°C, SA/V = 1.0
50
40
30
20
10
0
40
30
20
10
1200
1000
800
600
400
Wave number (cm⁻¹)

Figure 2

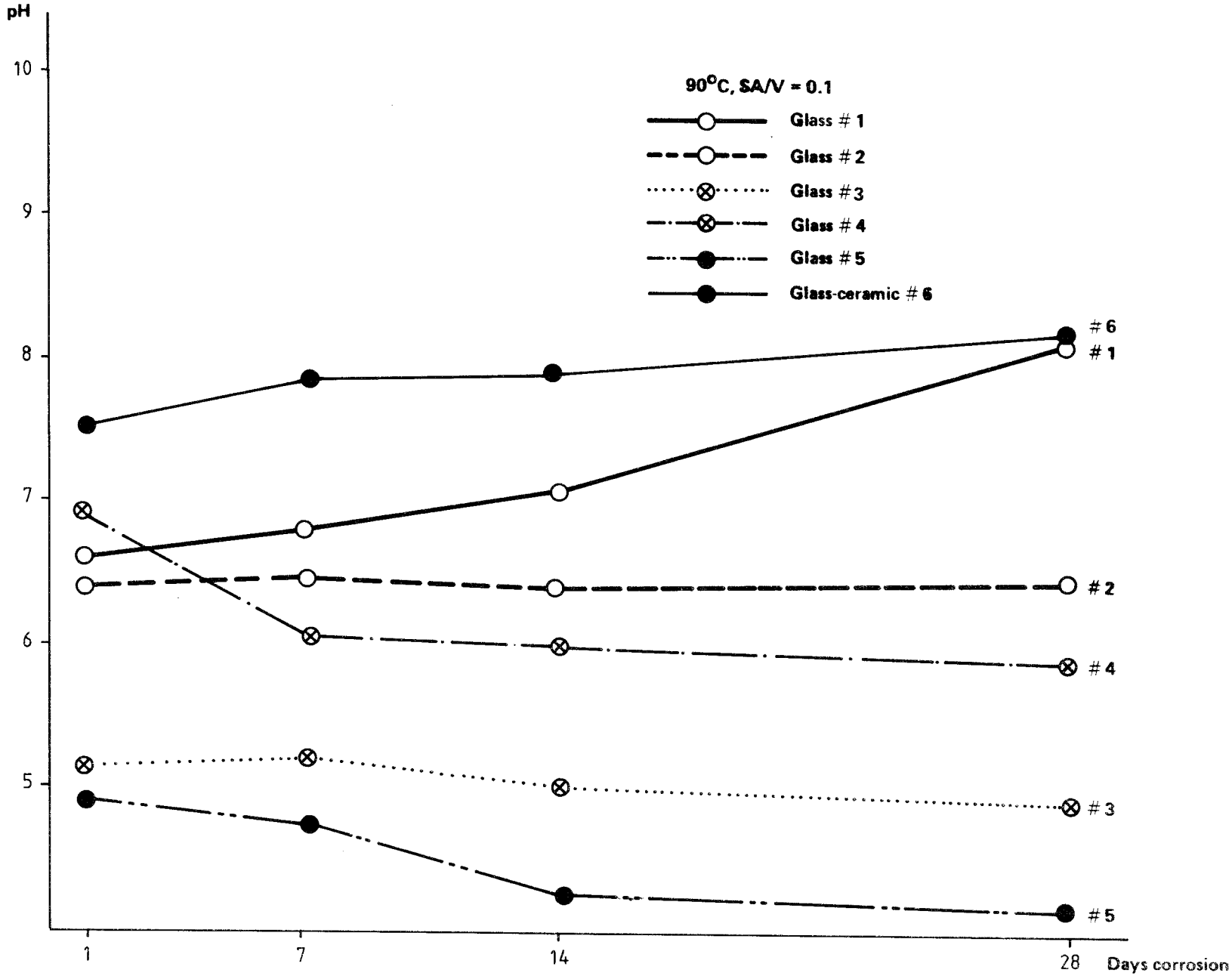
pH
10
9
8
7
6
5
90°C, SA/V = 0.1
Glass # 1
Glass # 2
Glass # 3
Glass # 4
Glass # 5
Glass-ceramic # 6
6
1
2
4
3
5
1
7
14
28
Days corrosion

Figure 3

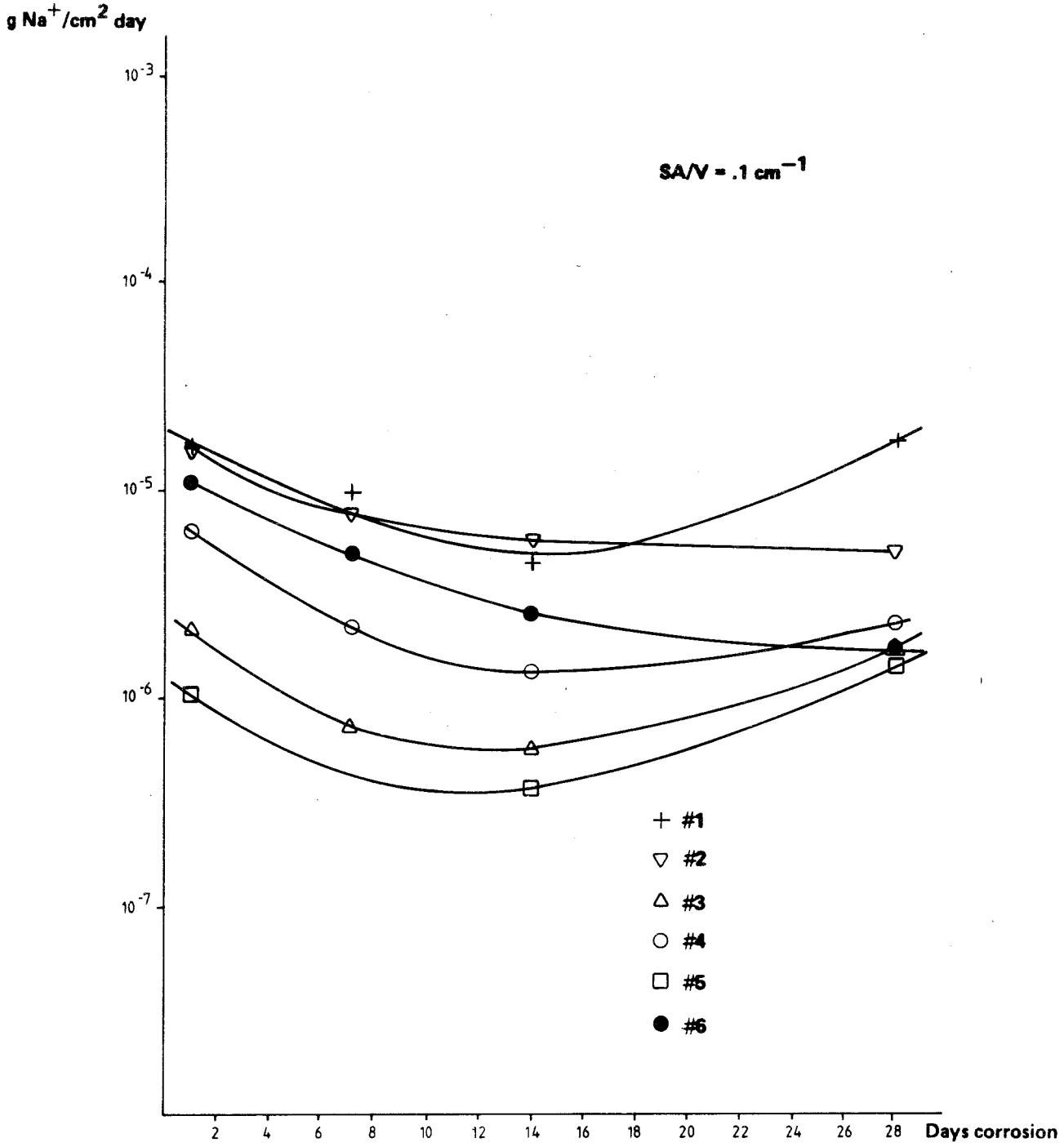
g Na+/cm2 day
10-3
10-4
10-5
10-6
10-7
SA/V = .1 cm-1
#1
#2
#3
#4
#5
#6
2
4
6
8
10
12
14
16
18
20
22
24
26
28
Days corrosion

Figure 4

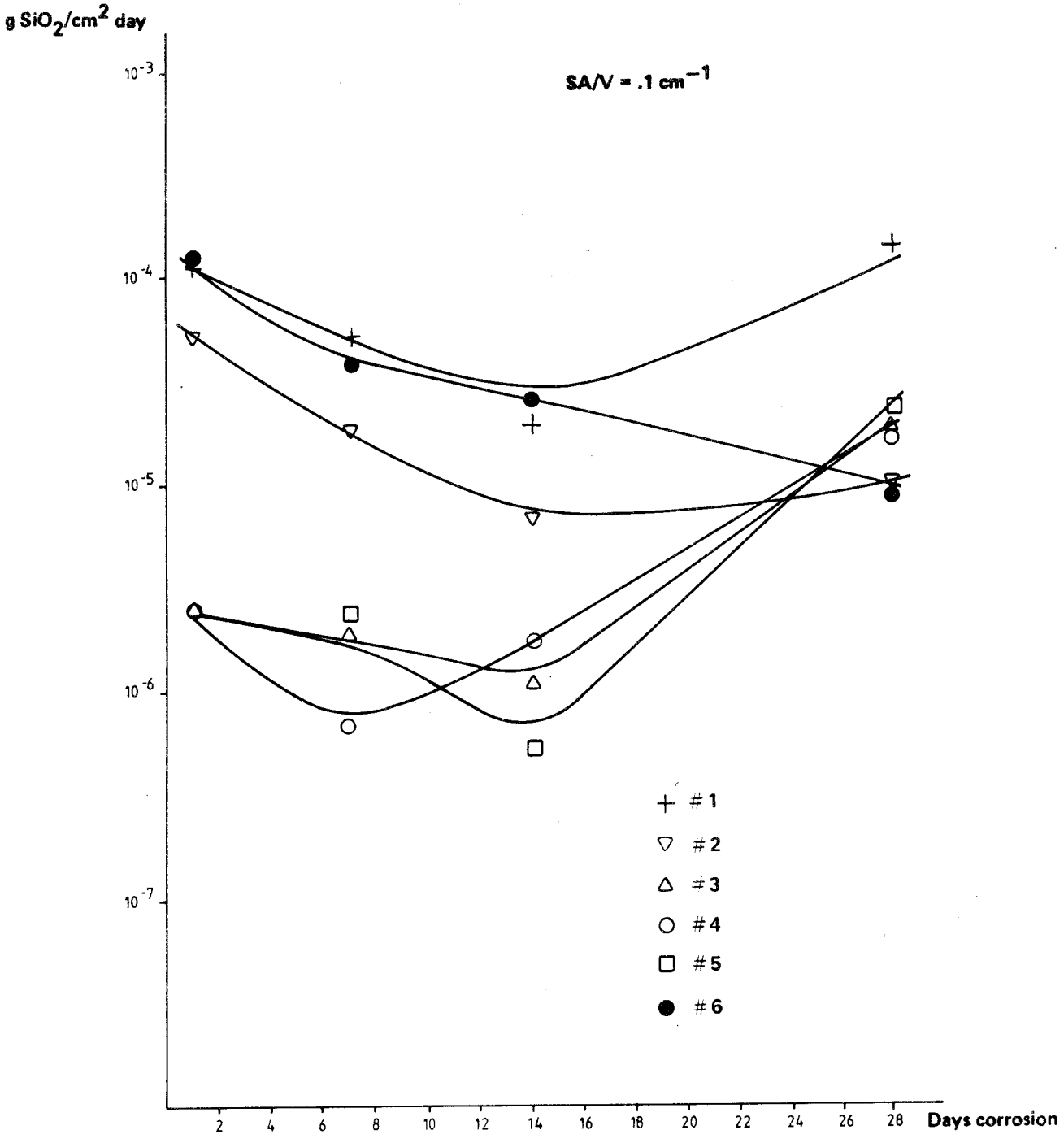
g SiO_2/cm^2 day
SA/V = .1 cm^{-1}
10^{-3}
10^{-4}
10^{-5}
10^{-6}
10^{-7}
2
4
6
8
10
12
14
16
18
20
22
24
26
28
Days corrosion
1
2
3
4
5
6

Figure 5

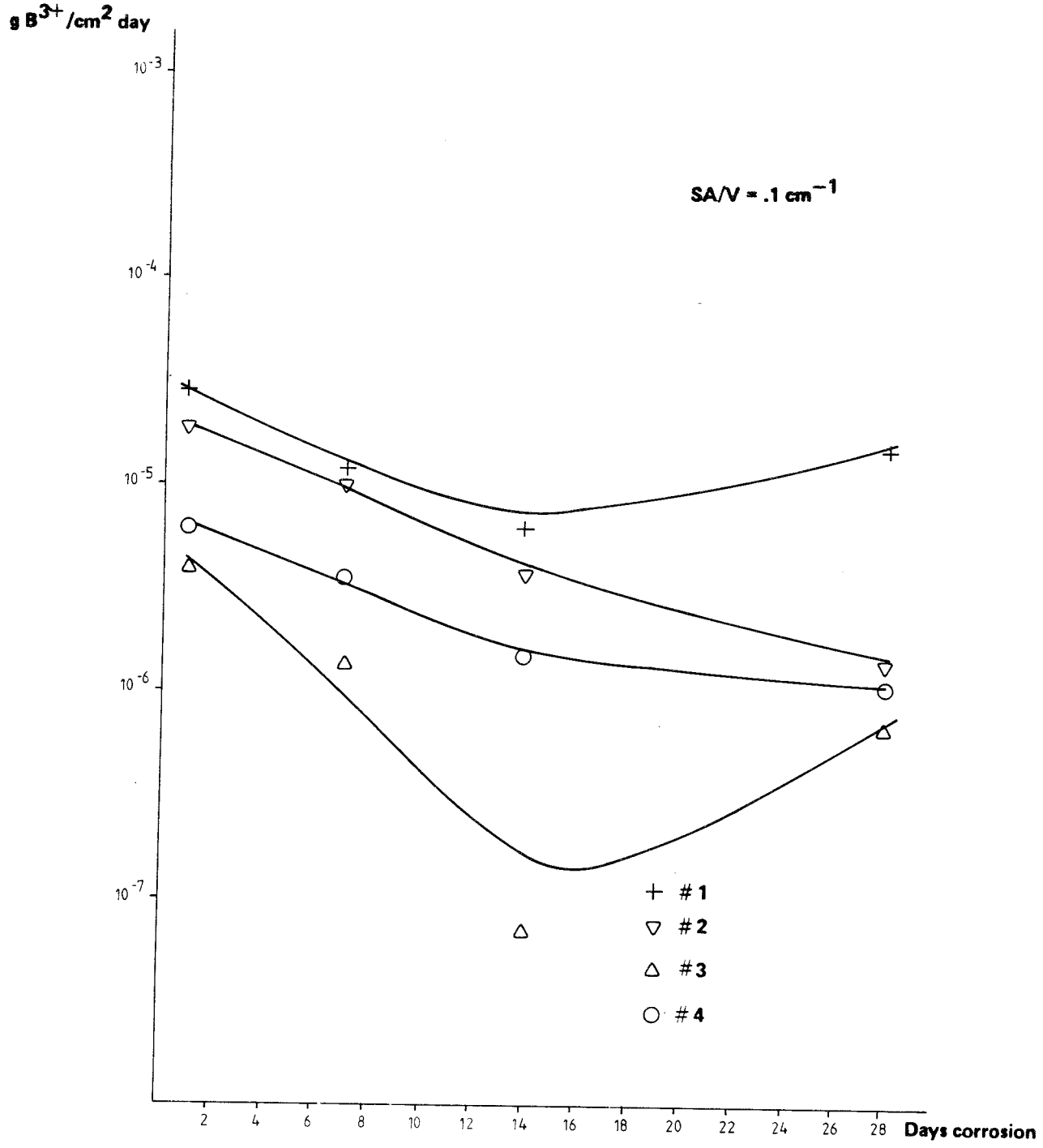
g B^{3+}/cm^2 day
10^{-3}
10^{-4}
10^{-5}
10^{-6}
10^{-7}
SA/V = .1 cm^{-1}
+ #1
▽ #2
△ #3
○ #4
2
4
6
8
10
12
14
16
18
20
22
24
26
28
Days corrosion

Figure 6

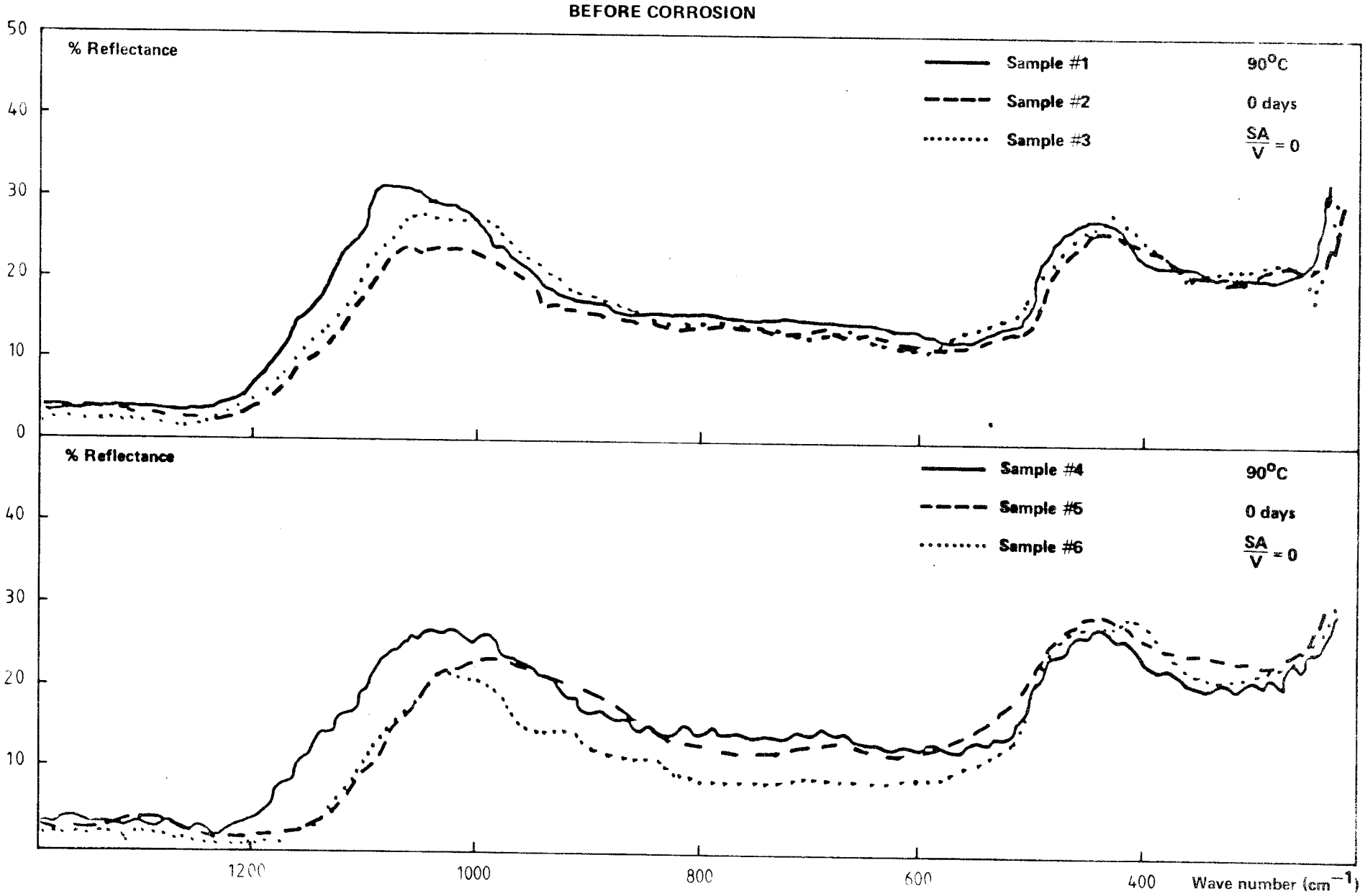
BEFORE CORROSION
% Reflectance
Sample #1
Sample #2
Sample #3
90°C
0 days
SA/V = 0
% Reflectance
Sample #4
Sample #5
Sample #6
90°C
0 days
SA/V = 0
50
40
30
20
10
0
1200
1000
800
600
400
Wave number (cm⁻¹)

Figure 7

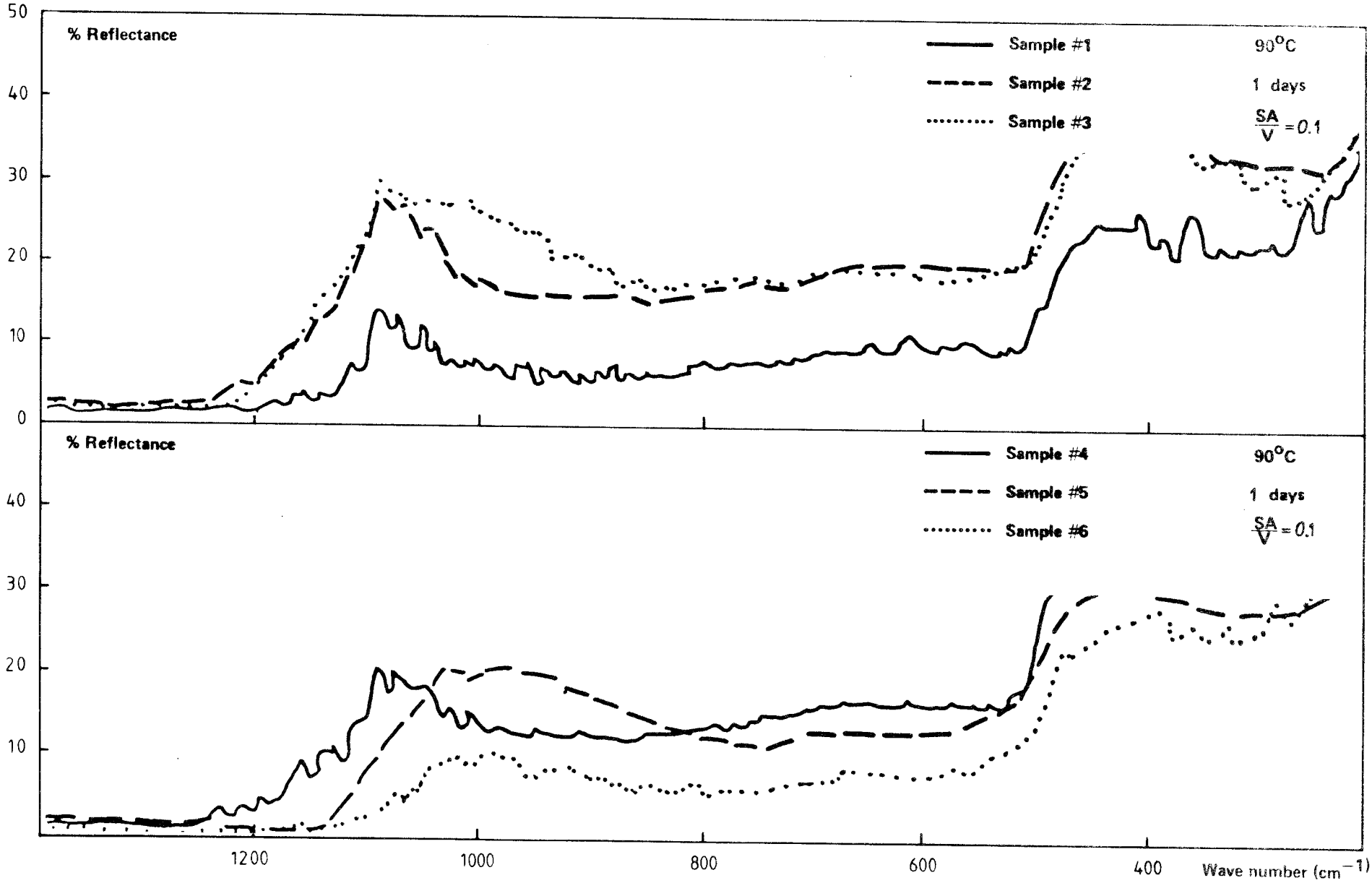
% Reflectance
Sample #1
Sample #2
Sample #3
90°C
1 days
SA/V = 0.1
% Reflectance
Sample #4
Sample #5
Sample #6
90°C
1 days
SA/V = 0.1
50
40
30
20
10
0
1200
1000
800
600
400
Wave number (cm⁻¹)

Figure 8

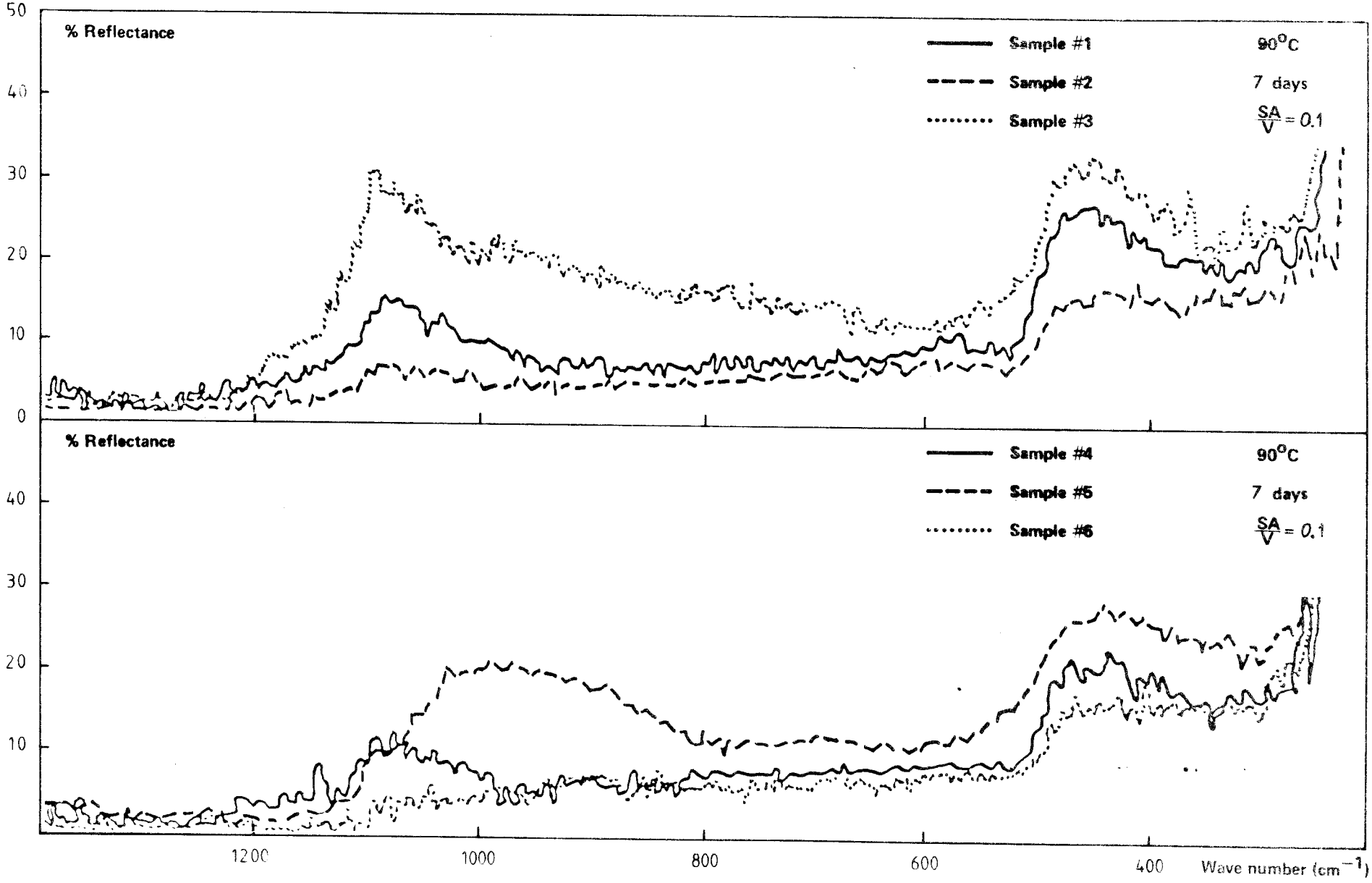
% Reflectance
Sample #1
Sample #2
Sample #3
90°C
7 days
SA/V = 0.1
% Reflectance
Sample #4
Sample #5
Sample #6
90°C
7 days
SA/V = 0.1
50
40
30
20
10
0
1200
1000
800
600
400
Wave number (cm⁻¹)

Figure 9

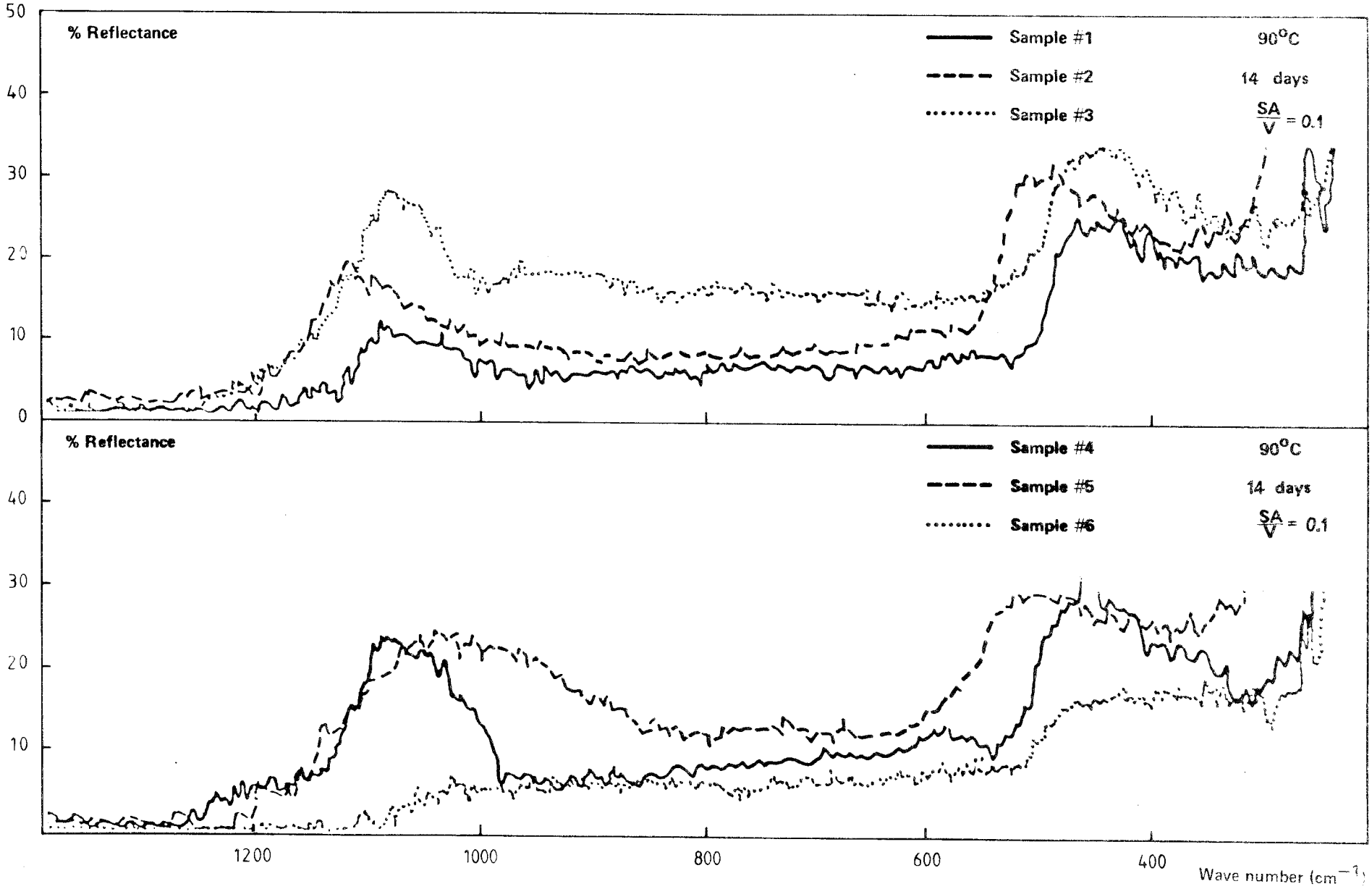
% Reflectance
Sample #1
Sample #2
Sample #3
90°C
14 days
SA/V = 0.1
% Reflectance
Sample #4
Sample #5
Sample #6
90°C
14 days
SA/V = 0.1
50
40
30
20
10
0
1200
1000
800
600
400
Wave number (cm⁻¹)

Figure 10

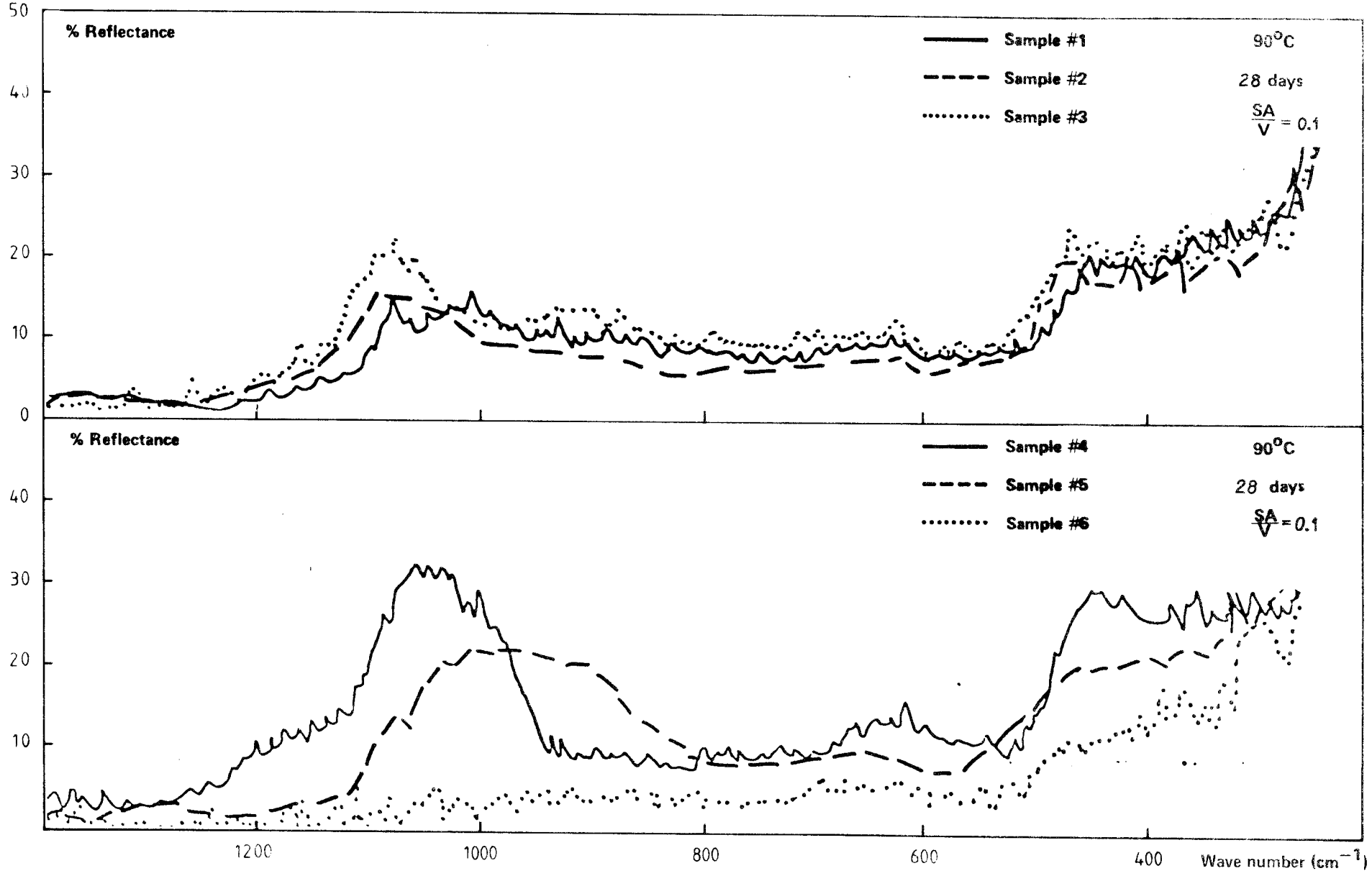
% Reflectance
Sample #1
Sample #2
Sample #3
90°C
28 days
SA/V = 0.1
% Reflectance
Sample #4
Sample #5
Sample #6
90°C
28 days
SA/V = 0.1
50
40
30
20
10
0
1200
1000
800
600
400
Wave number (cm⁻¹)

Figure 11

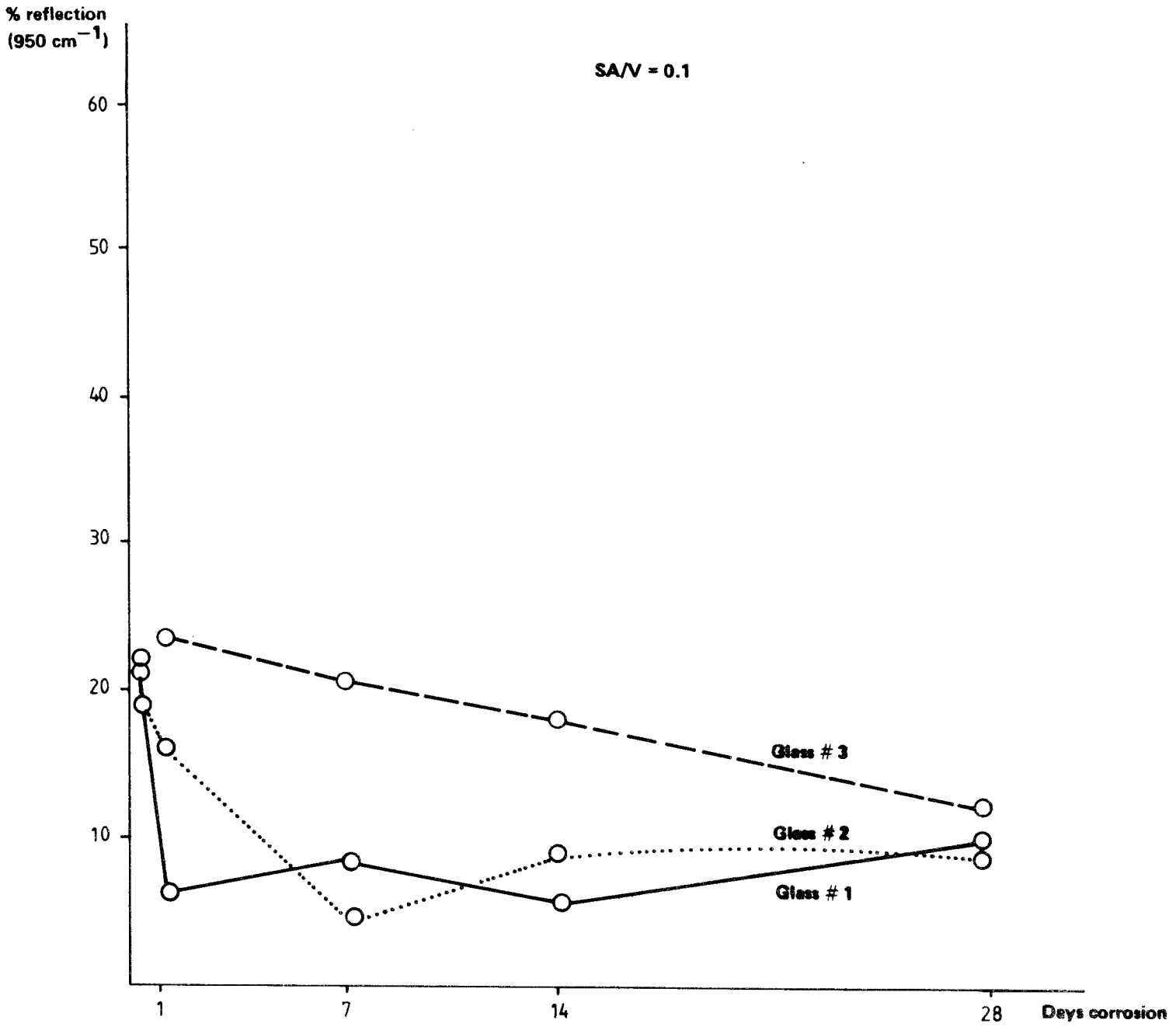
% reflection
(950 cm^{-1})
SA/V = 0.1
60
50
40
30
20
10
Glass # 3
Glass # 2
Glass # 1
1
7
14
28
Days corrosion

Figure 12

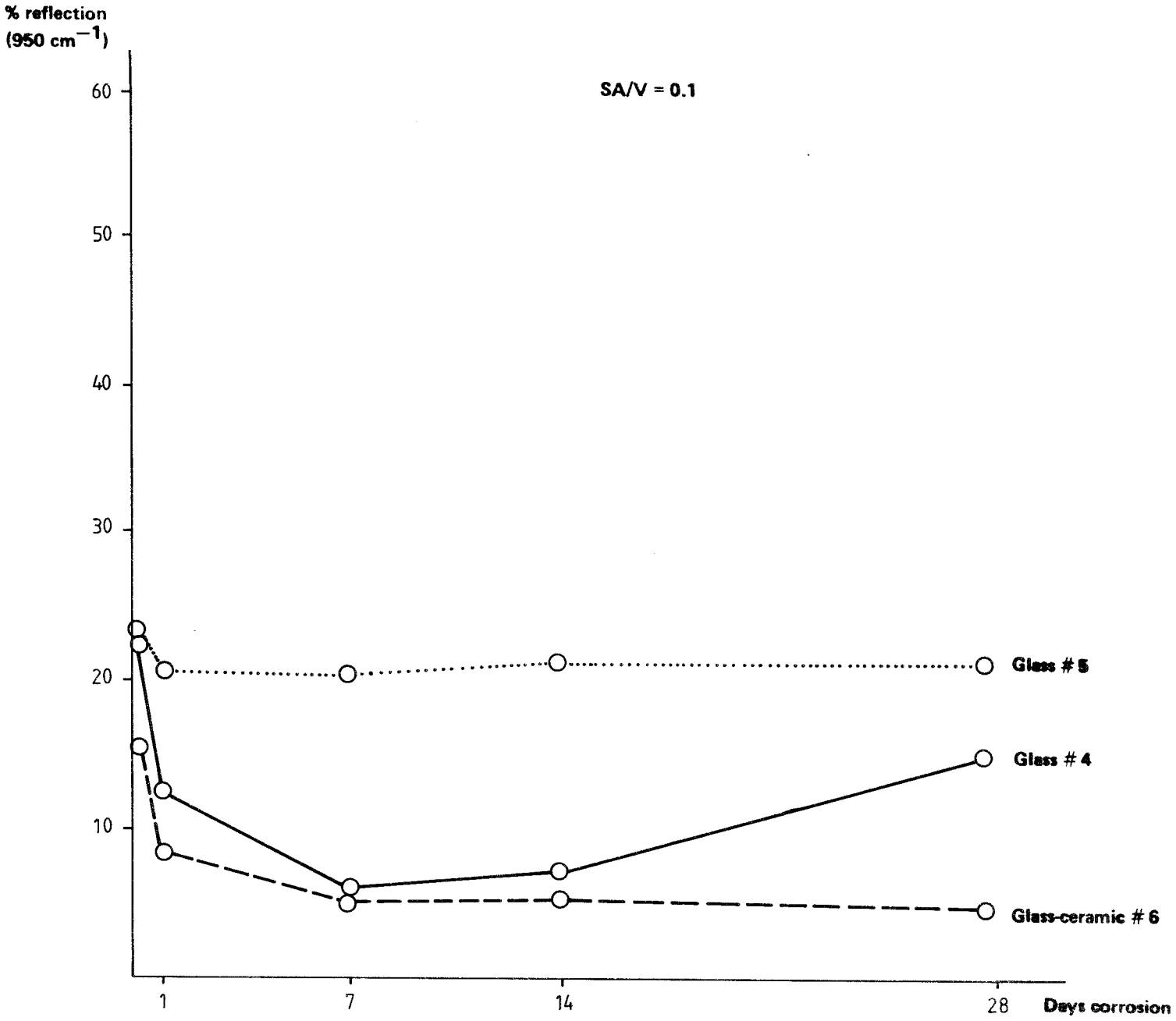
% reflection
(950 cm^{-1})
SA/V = 0.1
60
50
40
30
20
10
1
7
14
28
Days corrosion
Glass # 5
Glass # 4
Glass-ceramic # 6

Figure 13

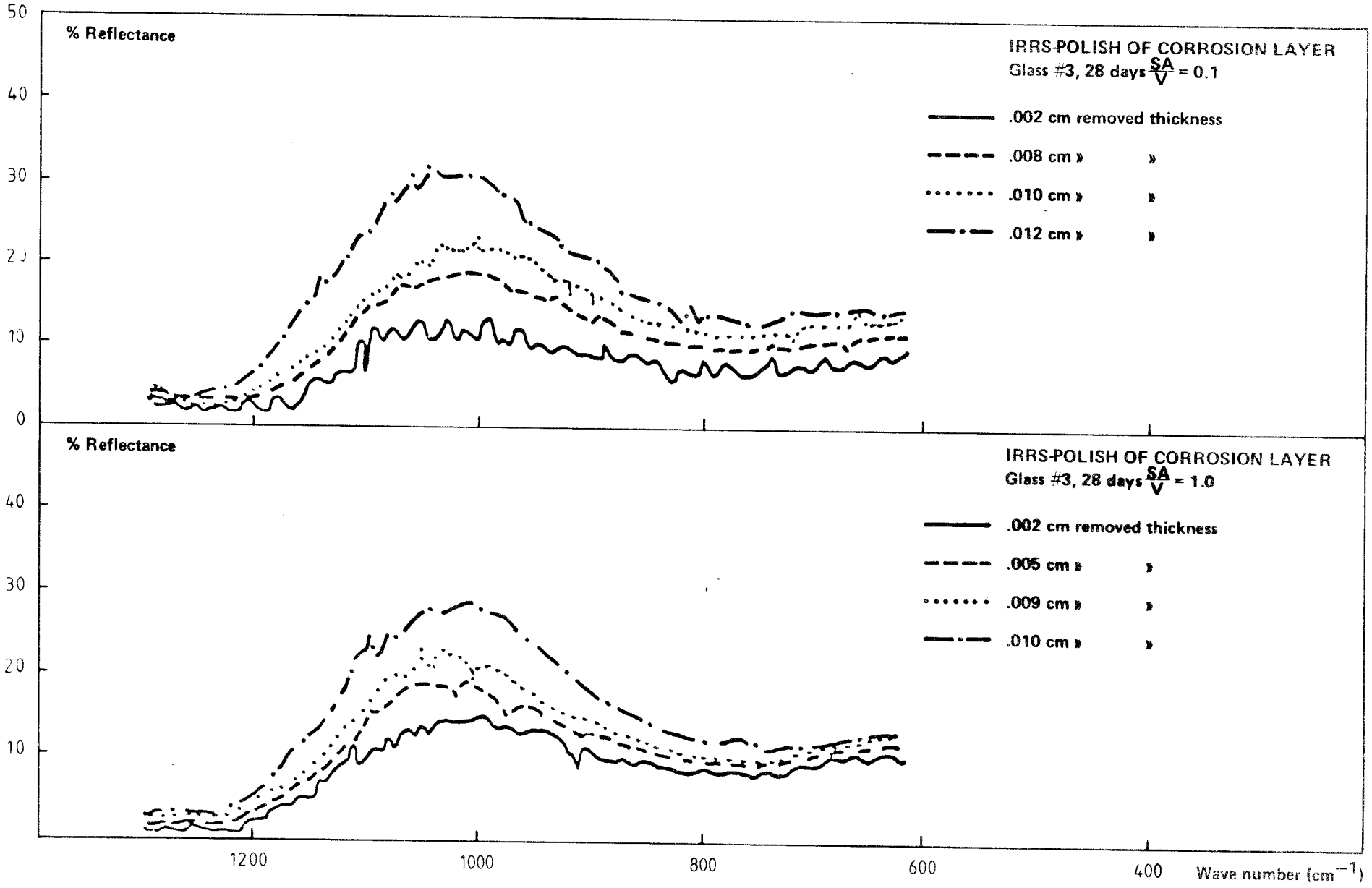
% Reflectance
IRRS-POLISH OF CORROSION LAYER
Glass #3, 28 days SA/V = 0.1
.002 cm removed thickness
.008 cm » »
.010 cm » »
.012 cm » »
% Reflectance
IRRS-POLISH OF CORROSION LAYER
Glass #3, 28 days SA/V = 1.0
.002 cm removed thickness
.005 cm » »
.009 cm » »
.010 cm » »
50
40
30
20
10
0
40
30
20
10
1200
1000
800
600
400
Wave number (cm⁻¹)

Figure 14

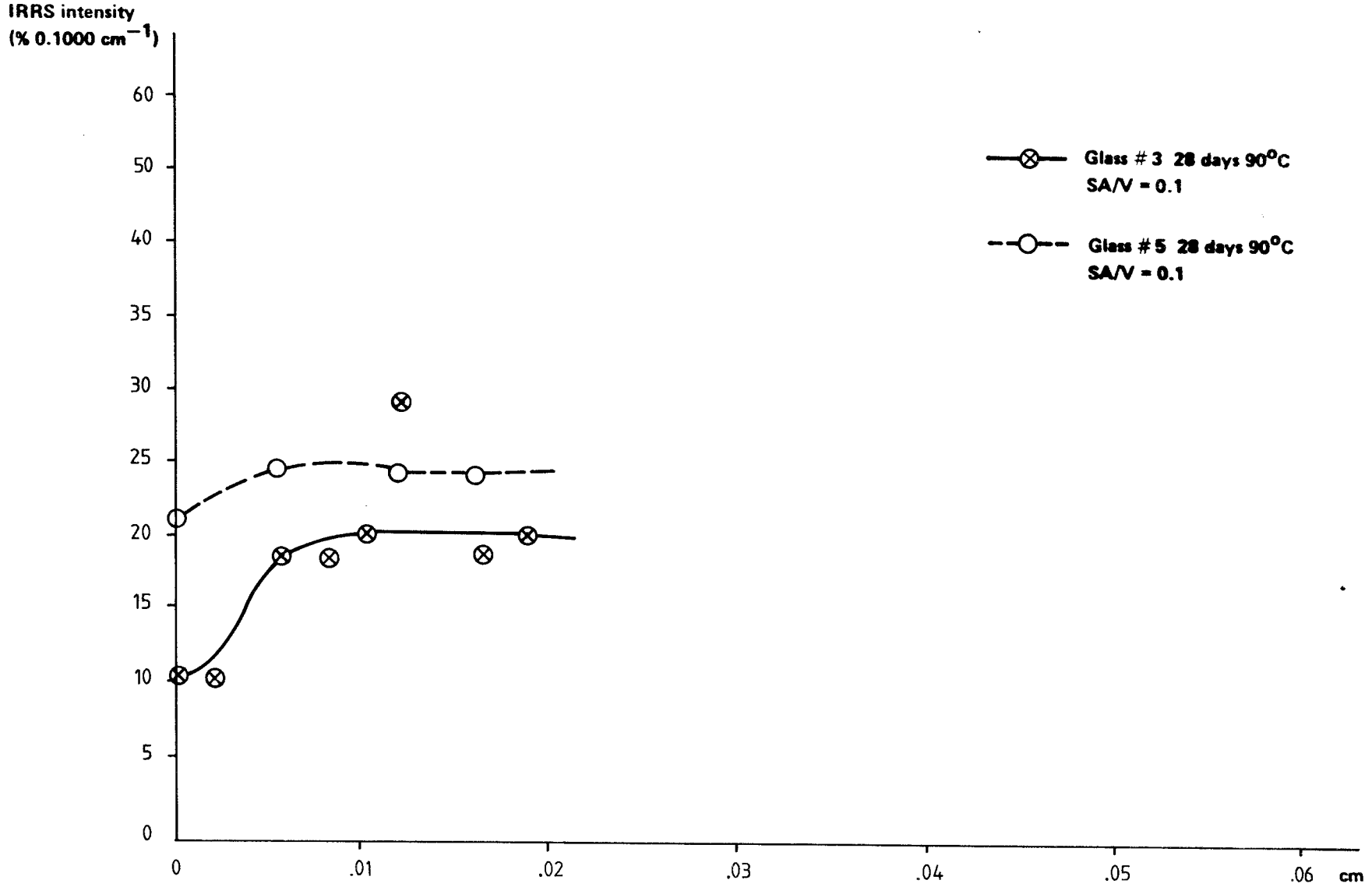
IRRS intensity
(% 0.1000 cm^{-1})
60
50
40
35
30
25
20
15
10
5
0
0
.01
.02
.03
.04
.05
.06
cm
Glass # 3 28 days 90°C
SA/V = 0.1
Glass # 5 28 days 90°C
SA/V = 0.1

Figure 15

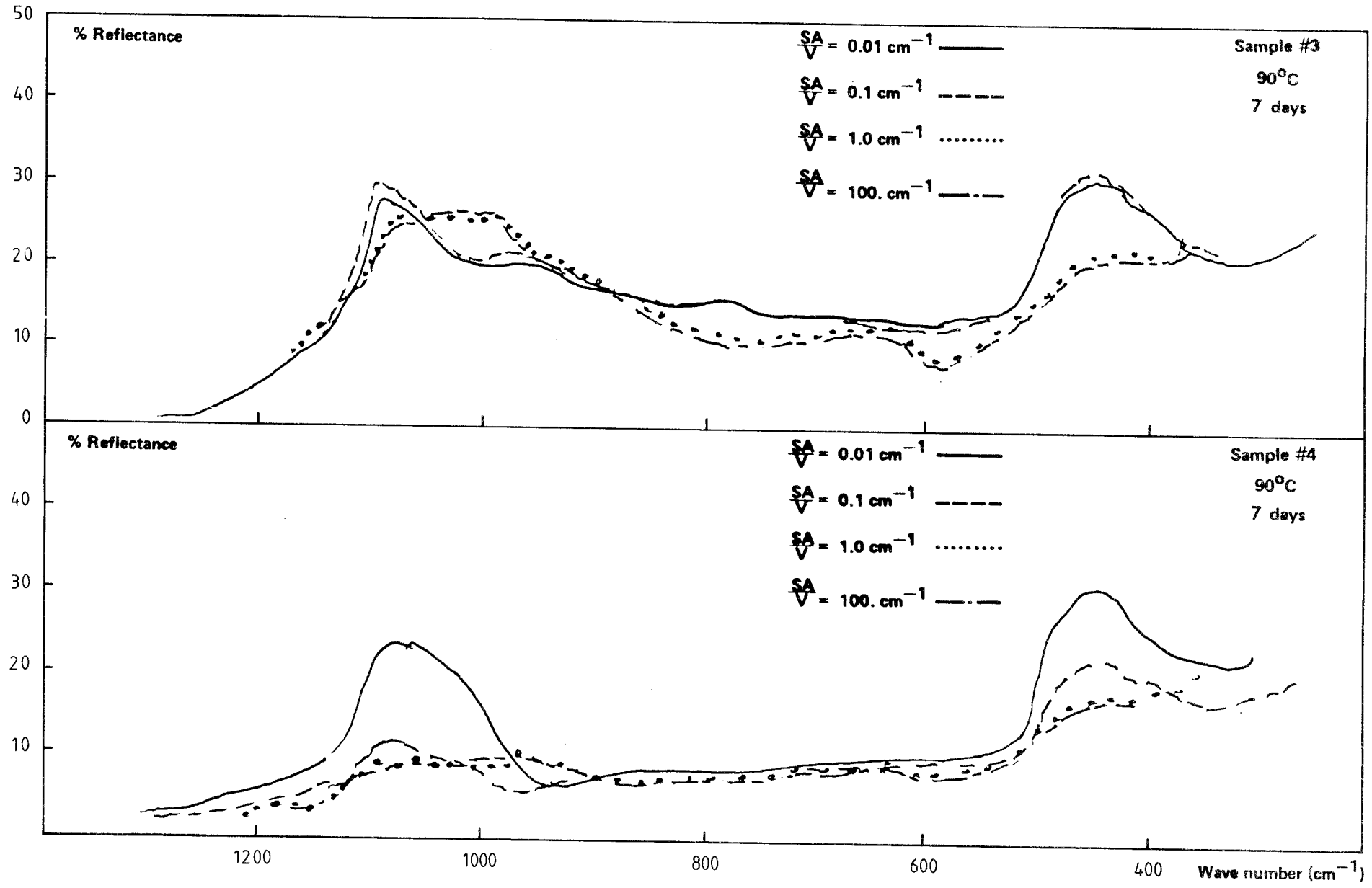
% Reflectance
SA/V = 0.01 cm⁻¹
SA/V = 0.1 cm⁻¹
SA/V = 1.0 cm⁻¹
SA/V = 100. cm⁻¹
Sample #3
90°C
7 days
% Reflectance
SA/V = 0.01 cm⁻¹
SA/V = 0.1 cm⁻¹
SA/V = 1.0 cm⁻¹
SA/V = 100. cm⁻¹
Sample #4
90°C
7 days
50
40
30
20
10
0
40
30
20
10
1200
1000
800
600
400
Wave number (cm⁻¹)

Figure 16

FÖRTECKNING ÖVER KBS TEKNISKA RAPPORTER

1977-78

TR 121 KBS Technical Reports 1 - 120.
Summaries. Stockholm, May 1979.

1979

TR 79-28 The KBS Annual Report 1979.
KBS Technical Reports 79-01--79-27.
Summaries. Stockholm, March 1980.

1980

TR 80-01 Komplettering och sammanfattning av geohydrologiska undersökningar inom sternöområdet, Karlshamn
Lennart Ekman
Bengt Gentzschein
Sveriges geologiska undersökning, mars 1980

TR 80-02 Modelling of rock mass deformation for radioactive waste repositories in hard rock
Ove Stephansson
Per Jonasson
Department of Rock Mechanics
University of Luleå

Tommy Groth
Department of Soil and Rock Mechanics
Royal Institute of Technology, Stockholm
1980-01-29

TR 80-03 GETOUT - a one-dimensional model for groundwater transport of radionuclide decay chains
Bertil Grundfelt
Mark Elert
Kemakta konsult AB, January 1980

TR 80-04 Helium retention
Summary of reports and memoranda
Gunnar Berggren
Studsvik Energiteknik AB, 1980-02-14

TR 80-05 On the description of the properties of fractured rock using the concept of a porous medium
John Stokes
Royal Institute of Technology, Stockholm
1980-05-09

TR 80-06 Alternativa ingjutningstekniker för radioaktiva jonbytarmassor och avfallslösningar
Claes Thegerström
Studsvik Energiteknik AB, 1980-01-29

TR 80-07 A calculation of the radioactivity induced in PWR cluster control rods with the origen and casmo codes
Kim Ekberg
Studsvik Energiteknik AB, 1980-03-12

TR 80-08 Groundwater dating by means of isotopes
A brief review of methods for dating old groundwater by means of isotopes
A computing model for carbon - 14 ages in groundwater
Barbro Johansson
Naturgeografiska Institutionen
Uppsala Universitet, August 1980

TR 80-09 The Bergshamra earthquake sequence of December 23, 1979
Ota Kulhánek, Norris John, Klaus Meyer, Torild van Eck and Rutger Wahlström
Seismological Section, Uppsala University
Uppsala, Sweden, August 1980

TR 80-10 Kompletterande permeabilitetsmätningar i finnsjö-området
Leif Carlsson, Bengt Gentzschein, Gunnar Gidlund, Kenth Hansson, Torbjörn Svenson, Ulf Thoregren
Sveriges geologiska undersökning, Uppsala, maj 1980

TR 80-11 Water uptake, migration and swelling characteristics of unsaturated and saturated, highly compacted bentonite
Roland Pusch
Luleå 1980-09-20
Division Soil Mechanics, University of Luleå

TR 80-12 Drilling holes in rock for final storage of spent nuclear fuel
Gunnar Nord
Stiftelsen Svensk Detonikforskning, september 1980

TR 80-13 Swelling pressure of highly compacted bentonite
Roland Pusch
Division Soil Mechanics, University of Luleå
Luleå 1980-08-20

TR-80-14 Properties and long-term behaviour of bitumen and radioactive waste-bitumen mixtures
Hubert Eschrich
Eurochemic, Mol, October 1980

TR 80-15 Aluminium oxide as an encapsulation material for unreprocessed nuclear fuel waste - evaluation from the viewpoint of corrosion
Final Report 1980-03-19
Swedish Corrosion Institute and its reference group

TR 80-16 Permeability of highly compacted bentonite
Roland Pusch
Division Soil Mechanics, University of Luleå
1980-12-23

TR 80-17 Input description for BIOPATH
Jan-Erik Marklund
Ulla Bergström
Ove Edlund
Studsvik Energiteknik AB, 1980-01-21

TR 80-18 Införande av tidsberoende koefficientmatriser i BIOPATH
Jan-Erik Marklund
Studsvik Energiteknik AB, januari 1980

TR 80-19 Hydrothermal conditions around a radioactive waste repository
Part 1 A mathematical model for the flow of groundwater and heat in fractured rock
Part 2 Numerical solutions
Roger Thunvik
Royal Institute of Technology, Stockholm, Sweden
Carol Braester
Israel Institute of Technology, Haifa, Israel
December 1980

TR 80-20 BEGAFIP. Programvård, utveckling och benchmarkberäkningar
Göran Olsson
Peter Hägglöf
Stanley Svensson
Studsvik Energiteknik AB, 1980-12-14

TR 80-21 Report on techniques and methods for surface characterization of glasses and ceramics
Bengt Kasemo
Mellerud, August 1980

TR 80-22 Evaluation of five glasses and a glass-ceramic for solidification of Swedish nuclear waste
Larry L Hench
Ladawan Urwongse
Ceramics Division
Department of Materials Science and Engineering
University of Florida, Gainesville, Florida
1980-08-16

TR 80-23 Exact solution of a model for diffusion in particles and longitudinal dispersion in packed beds
Anders Rasmuson
Ivars Neretnieks
Royal Institute of Technology, August 1979

TR 80-24 Migration of radionuclides in fissured rock - The influence of micropore diffusion and longitudinal dispersion
Anders Rasmuson
Ivars Neretnieks
Royal Institute of Technology, December 1979

TR 80-25 Diffusion and sorption in particles and two-dimensional dispersion in a porous media
Anders Rasmuson
Royal Institute of Technology, January 1980